Advanced Carbon Capture
for steel industries integrated in CCUS Clusters

Innovation Action

This project has received funding from the European Union's Horizon 2020 research and innovation programme under the Grant Agreement No 884418.

D2.6 Experimental results of alternative reactor schemes for CASOH process

Work Package: 2
Due date of deliverable: month 40
Actual submission date: 17 /July / 2023
Start date of project: 1 / April / 2020
Duration: 48 months
Lead beneficiary for this deliverable: CANMET (associated partner to UCL)
Contributors: Yewen Tan (CANMET), Dennis Lu (CANMET), Nicole Bond (CANMET), José Ramón Fernández (CSIC), Miriam Díaz (CSIC), Gemma Grasa (CSIC), Alberto Méndez (CSIC), Borja Arias (CSIC), Carlos Abanades (CSIC),
Reviewer: Vincenzo Spallina (UNIMAN)

Dissemination Level: **PU**

Contents

*This project has received funding from the European Union's Horizon 2020 research and innovation programme under the Grant Agreement No **884418***

1. Version log

Version	Date	Released by	Nature of Change
0.1	21/04/2023	Carlos Abanades	Scope and first draft
0.2	1/06/2023	Gemma Grasa	ICB-CSIC; steam calcination
0.3	12/06/2023	Nicole Bond	CANMET contribution
0.4	21/06/2023	JR Fernandez/M Díaz	First full draft for review
1.0	13/07/2023	V Spallina	UMAN; Revision

*This project has received funding from the European Union's Horizon 2020 research and innovation programme under the Grant Agreement No **884418***

2. Definition and acronyms

Acronyms	Definitions
BFG	Blast Furnace Gas
CASOH	Calcium Assisted Steel-mill Off-gas Hydrogen
CLC	Chemical Looping Combustion
LHV	Low Calorific Value
TGA	Thermo-gravimetric Analysis
WGS	Water Gas Shift
PTGA	Pressurized thermogravimetric analyzer
PCL	Pressurized chemical looping test
TRL	Technology Readiness Level
MS	Mass spectrometer
CaL	Calcium Looping
SCM	Shrinking Core Model

*This project has received funding from the European Union's Horizon 2020 research and innovation programme under the Grant Agreement No **884418***

3. Summary of the Report

This deliverable presents the results from the investigations of two reactor systems of potential use to decarbonize steel-mill off gases using high temperature solid looping cycles. These approaches represent alternative reactor schemes and heat management strategies respect to the CASOH process adopted for demonstration at TRL7 in WP2 of the C^{4}U project.

The main achievements from these works are summarized in the following points:

1) CANMET/NRCAN has obtained a first proof of concept at TRL4 of the viability of fluidised bed reactor to efficiently burn CH4 containing gases (i.e. a proxy of Coke Oven Gas) at high pressure using a Cu-containing oxygen carrier as fluidizing media. However, since the stability of operation has been challenging and the conversion of the fuel gases uncomplete in the test conducted so far, we maintain in WP2 the priority interest in demonstrating at TRL7 the packed bed reactor approach initially adopted in the C^{4}U project.
2) CSIC has adapted to the CASOH process boundary conditions (i.e. mainly targeting decarbonisation of BFG in packed beds by Ca-based sorption enhanced water gas shift) an alternative heat management strategy based on pressure swing sorption/desorption process, involving calcination assisted by vacuum and/or by feeding of steam. New experimental evidence in different test rigs, has provided support for such strategy in CASOH applications.
3) The extraction of ultrapure CO_2 from the calcination stage of $CaCO_3$ when vacuum is applied to a preheated bed of solids containing $CaCO_3$ has been experimentally demonstrated at TRL3. Steam assisted calcination can also yield similar results, after water condensation.
4) Adiabatic cooling caused in the bed during calcination by CO_2 partial pressure swings opens up new opportunities for heat management in the CASOH process, drastically reducing the duration of heat removal stages and increasing the yields of H_2.
5) Simulations with the reactor model available for CASOH reactions confirms viability of the new approaches and its potential advantages at large scale respect to the original version of the CASOH process relying on the intense use of heat removal stages. These promising results have affected priorities in the full process simulations and technoeconomic analysis ongoing in WP3, that is being reconsidered/adapted to fully exploit at large scale the new findings reported in this deliverable.

*This project has received funding from the European Union's Horizon 2020 research and innovation programme under the Grant Agreement No **884418***

4. Introduction and scope

This public deliverable D2.6 is part of work package 2 of the C⁴U project (1). The main objective in WP2 is the experimental demonstration at TRL7 of the CASOH process *("Calcium Assisted Steel mill Off-gas Hydrogen production")*. This process is a CO_2 capture technology designed to produce H_2 and heat from steel mill off-gases that contain CO, such as blast furnace gas (BFG), which is today a major source of carbon (in the form of CO and CO_2) in integrated steel mills. Figure 1 represents the basic scheme the initial CASOH process proposed in C⁴U.

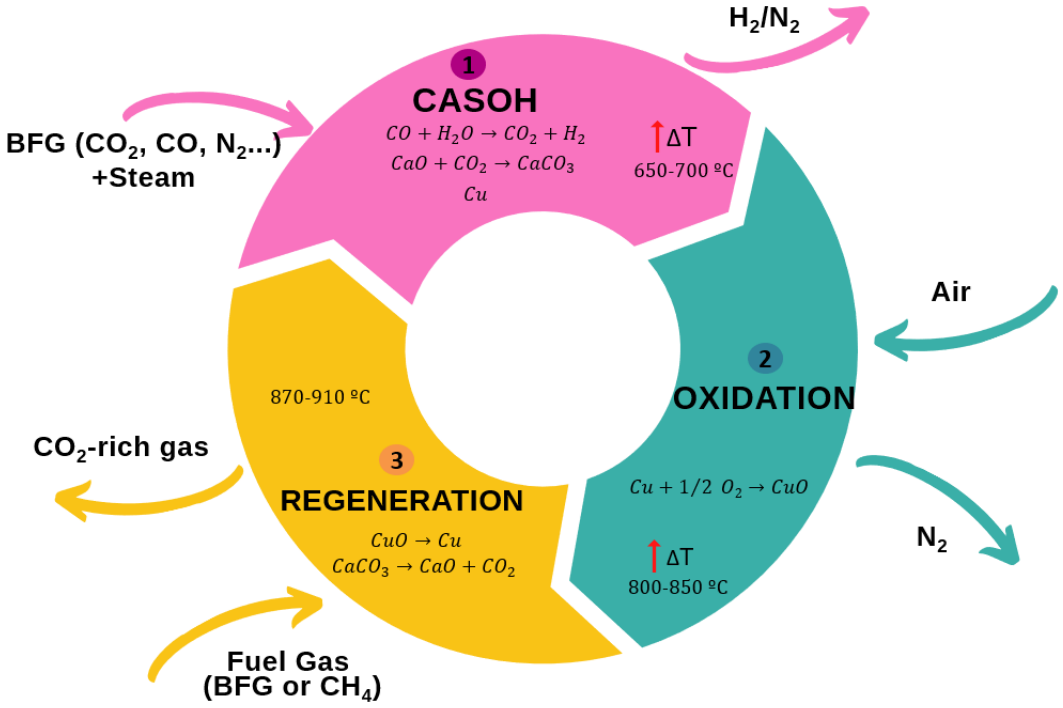

Figure 1. Scheme of the CASOH process for the production of H_2/N_2 from BFG with CO_2 capture.

The process relies on high-temperature reversible solid looping reactions of carbonation/calcination reactions of $CaO/CaCO_3$ and oxidation/reduction reactions of Cu/CuO. Separately, these reversible gas-solid reaction loops have been extensively investigated in a wide variety of calcium looping systems for CO_2 capture (2,3) as well as in chemical looping combustion systems (4). The combination of these reactions in a single bed of solids has also been studied for sorption enhanced reforming applications within the EU Ascent project (5,6). Based on this background, the CASOH process for BFG was conceived as a system containing the functional Ca-Cu material in a packed-bed reactor that continuously switches between three reaction stages, as shown in Figure 1. In a first "CASOH" stage, CaO captures the CO_2 through carbonation, including the CO_2 formed by the catalyzed Water Gas

*This project has received funding from the European Union's Horizon 2020 research and innovation programme under the Grant Agreement No **884418***

Shift (WGS) reaction of CO present in the BFG (i.e. calcium-assisted sorption-enhanced water gas shift reaction). In a second reaction stage, the Cu-based WGS catalyst/oxygen carrier undergoes oxidation with air. Finally, in the third stage, there is the exothermic reduction of CuO with a fuel gas driving the decomposition of $CaCO_3$, generating a concentrated CO_2 gas stream, and regenerating the CaO used in the first reaction stage.

The experimental proof of concept at TRL≤4 for the reactions shown in Figure 3.1 has been already published in the open literature by C⁴U project partners (5,7), and such concept remains a key target for demonstration at TRL7 (8,9). However, since the CASOH technology is still in its development, it was recognised during the project preparation stage that other process variants and reactor choices (i.e. fluidised beds vs packed bed approaches), could still be explored while relying on the inherent benefits of high-temperature solid looping reactions to capture CO_2 from the characteristic fuel gases in a steel mill. Therefore, the C⁴U workplan includes parallel research activities to explore alternative heat management strategies in the CASOH process, involving novel approaches to reduce the energy demand during the regeneration stage. This includes the introduction of vacuum swings or other forms of pressure swings, following similar process principles in solid-sorbent based systems operating at lower temperatures. This deliverable reports the progress made in C⁴U regarding the development of such tasks.

On the other hand, the EU Call Text addressed by the C⁴U project, including an invitation to enhance international collaborations EU/Canada. Given the existing collaboration between CANMET/NRCAN and CSIC in high-temperature looping cycles, and ongoing work at CANMET/NRCAN developing fluidised bed-based chemical looping combustion technologies of fuel gases, including steel-ill off-gases (BFG, COG, etc), CANMET/NRCAN was included in the project consortium (formally as Associated Partner of the project coordinator, UCL). This addition brings to the C⁴U consortium additional expertise and research activities to benchmark the high-temperature processes under development in WP2. Potentially, the high-pressure CLC fluidised bed approach under investigation at CANMET/NRCAN offers an alternative reactor choice to the packed bed technologies explored by other WP2 partners at TRL7 in C⁴U.

In this Deliverable 2.6, we report in section 4 the progress made at CANMET/NRCAN in their development of a fluidized bed experimental test facility to test high-temperature solid looping processes when burning CH4, which could serve as a proxy for COG and other fuel gases from steelmaking processes. Additionally, in section 5 we present the first experimental proof of concept of a novel reactor design by CSIC aimed at improving the heat management of the reference CASOH process by introducing a vacuum swing (or CO_2 partial pressure swing with steam) $CaCO_3$ calcination stage to the high-temperature looping reactions in CASOH.

*This project has received funding from the European Union's Horizon 2020 research and innovation programme under the Grant Agreement No **884418***

5. CANMET´s activities towards the design and commissioning of a high pressure fluidized bed reactor for high temperature solid looping cycles

CanmetENERGY has constructed and commissioned a bench-scale pressurized fluidized bed for testing reaction kinetics and characterizing the behaviour of candidate oxygen carriers for chemical looping combustion (CLC). This technology has the potential to be used for carbon capture and heat recovery within the iron and steel industry. The capabilities of this facility complement test work done via thermogravimetric analysis (TGA) in a more realistic reacting environment for chemical looping combustion.

The bench-scale fluidized bed facility comprises a pressure vessel with an internal compartment to house the fluidized bed, a gas supply system, an off-gas treatment system and a mass spectrometer for continuous off-gas analysis, as shown in Figure . The gas supply system enables the simultaneous delivery of mixtures of any combination of nitrogen, air, CO_2, or other mixed gas from a compressed gas cylinder. Mass flow controllers are utilized to easily control the on/off or modulation of gases, enabling them to pass through redox and purge cycles in the reactor. The reactor pressure is manually adjusted using a pressure letdown valve at the outlet of the reactor, prior to sampling, cooling and venting of the off-gas.

The reactor pressure vessel can operate up to a maximum temperature of 950 °C at 30 barg and is externally heated by a three-zone electric furnace (Figure A). An internal pipe sleeve with an internal diameter of 15.5 mm (Figure B) slides up inside the pressure vessel to form the reactor assembly (Figure C). A sintered metal filter, positioned 200 mm above the bottom of the heating zone of the furnace, acts as the gas distributor plate and provides a pre-heating zone for the fluidizing gas. The bed material (approximately 30 g, depending on the material) must be pre-loaded into the internal pipe sleeve before assembly of the pressure vessel. The fluidized bed and freeboard space have a length of 460 mm, and a second sintered metal filter is placed at the top to prevent solids from exiting the reactor.

*This project has received funding from the European Union's Horizon 2020 research and innovation programme under the Grant Agreement No **884418***

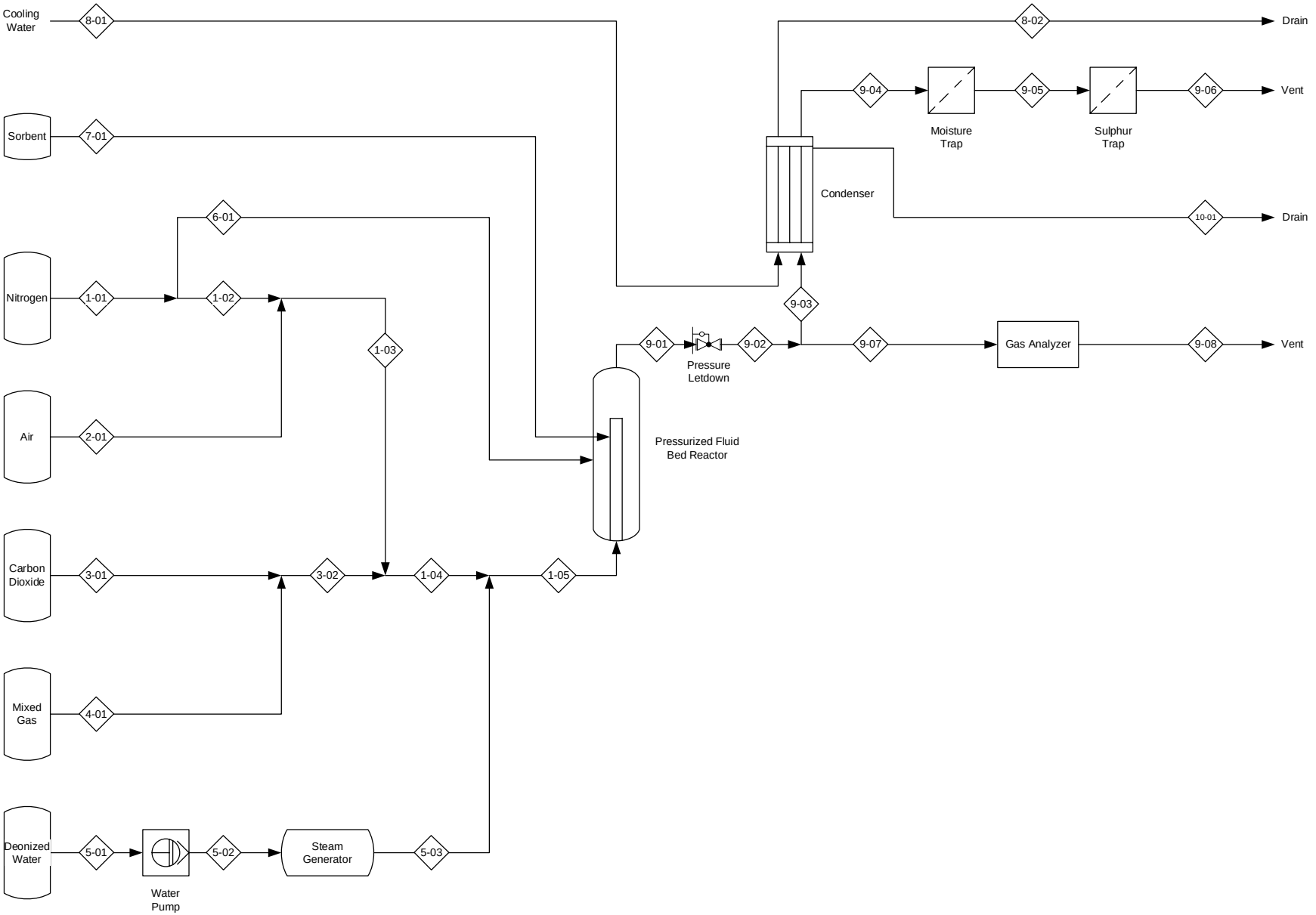

Figure 2. Process flow diagram for bench-scale fluidized bed facility.

*This project has received funding from the European Union's Horizon 2020 research and innovation programme under the Grant Agreement No **884418***

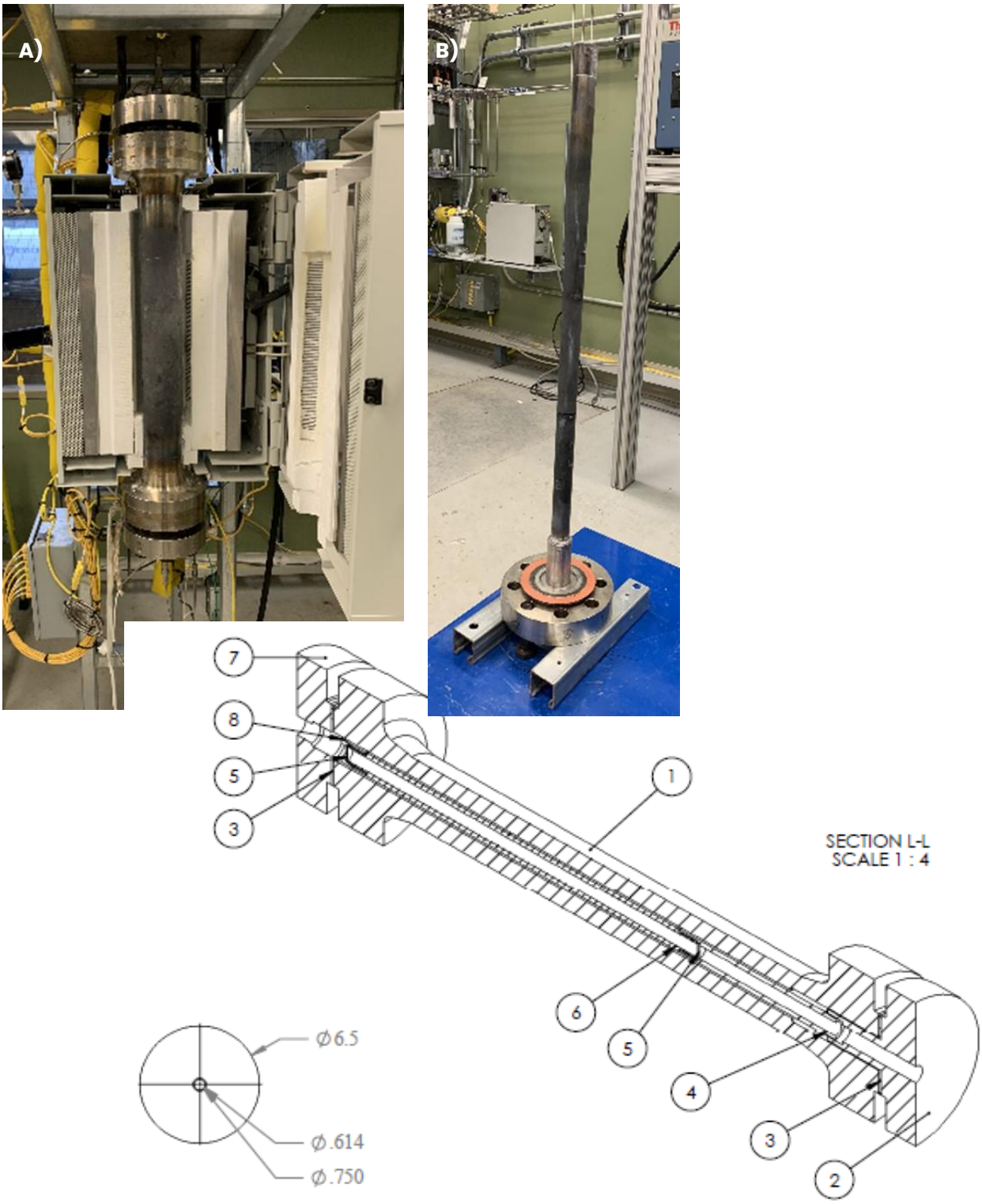

Figure 3. Reactor set up: A) Pressure vessel; B) Internal sleeve housing fluidized bed and distributor and C) Schematic of internal and external components.

*This project has received funding from the European Union's Horizon 2020 research and innovation programme under the Grant Agreement No **884418***

CanmetENERGY-Ottawa has been working with a collaborator to test their oxygen carrier in a fluidized bed operating under atmospheric pressure, using CH_4 and H_2/CO as fuels. Previously, CanmetENERGY-Ottawa has tested the oxygen carrier using both a pressurized TGA and an atmospheric pressure TGA with CH_4 as fuel. In order to support the design and engineering of a pilot-scale pressurized chemical looping (PCL) test facility being developed at CanmetENERGY-Ottawa, it is crucial to test this oxygen carrier under pressurized conditions using a fluidized bed.

This work aims to achieve the following objectives:

- Evaluate the performance of the oxygen carrier using a bench-scale pressurized fluidized bed.
- Investigate both oxidation and reduction reactions.
- Determine impact of reacting species partial pressure (i.e. O_2 for oxidation and CH_4 for reduction) and temperature on the apparent rate of reaction of the oxygen carrier.
- Determine the oxygen carrying capacity.
- Compare the kinetic results obtained with the fluidized bed set-up to those obtained using a pressurized thermogravimetric analyzer (PTGA).
- Validate the 2-phase 1D reactor model (developed by others).

To achieve the aforementioned objectives, tests were conducted as outlined in

Table 1. Test 1 considers the effects of the number of redox cycles, Tests 2-3 examine the effects of reactant (CH_4) partial pressure, Tests 4-5 investigate the effects of oxygen partial pressure, and Tests 7-9 explore the effects of temperature.

*This project has received funding from the European Union's Horizon 2020 research and innovation programme under the Grant Agreement No **884418***

Table 1. Completed tests and their test conditions.

NO.	Reduction Gases	Reduction Time, (min)	Oxidation gases	Oxidation Time, (min)	Pressure, (a. bar)	Temperature (°C)	U/Umf	Cycle No.
#1	CH_4/CO_2 (50/50)	20	Air/N_2 (50/50)	30	7	850	2	5, 10
#2	CH_4/CO_2 (25/75)	20	Air/N_2 (50/50)	30	7	850	2	5
#3	CH_4/CO_2 (10/90)	20	Air/N_2 (50/50)	30	7	850	2	5
#4	CH_4/CO_2 (50/50)	20	Air/N_2 (100/0)	30	7	850	2	5
#5	CH_4/CO_2 (50/50)	20	Air/N_2 (25/75)	30	7	850	2	5
#6	CH_4/CO_2 (50/50)	20	Air/N_2 (10/90)	30	7	850	2	5
#7	CH_4/CO_2 (50/50)	20	Air/N_2 (50/50)	30	7	850	2	10
#8	CH_4/CO_2 (50/50)	15	Air/N_2 (50/50)	35-60	7	925	2	10
#9	CH_4/CO_2 (50/50)	20	Air/N_2 (50/50)	30	7	775	2	10

An oxygen carrier containing Cu, Mn and Fe was used for this test series. Particles were sieved to a size range of 150-300 µm. They have a particle density of 3910 kg/m^3 and a bulk density of 2150 kg/m^3.

The tests were conducted using the bench-scale fluidized bed described above. Before the test campaign, commissioning tests were performed to obtain temperature profiles along the length inside the reactor above the distributor. The results are presented in Figure . As depicted, the actual temperature inside the reactor was about 40°C higher than the setpoint. A sintered disk was used as the distributor.

*This project has received funding from the European Union's Horizon 2020 research and innovation programme under the Grant Agreement No **884418***

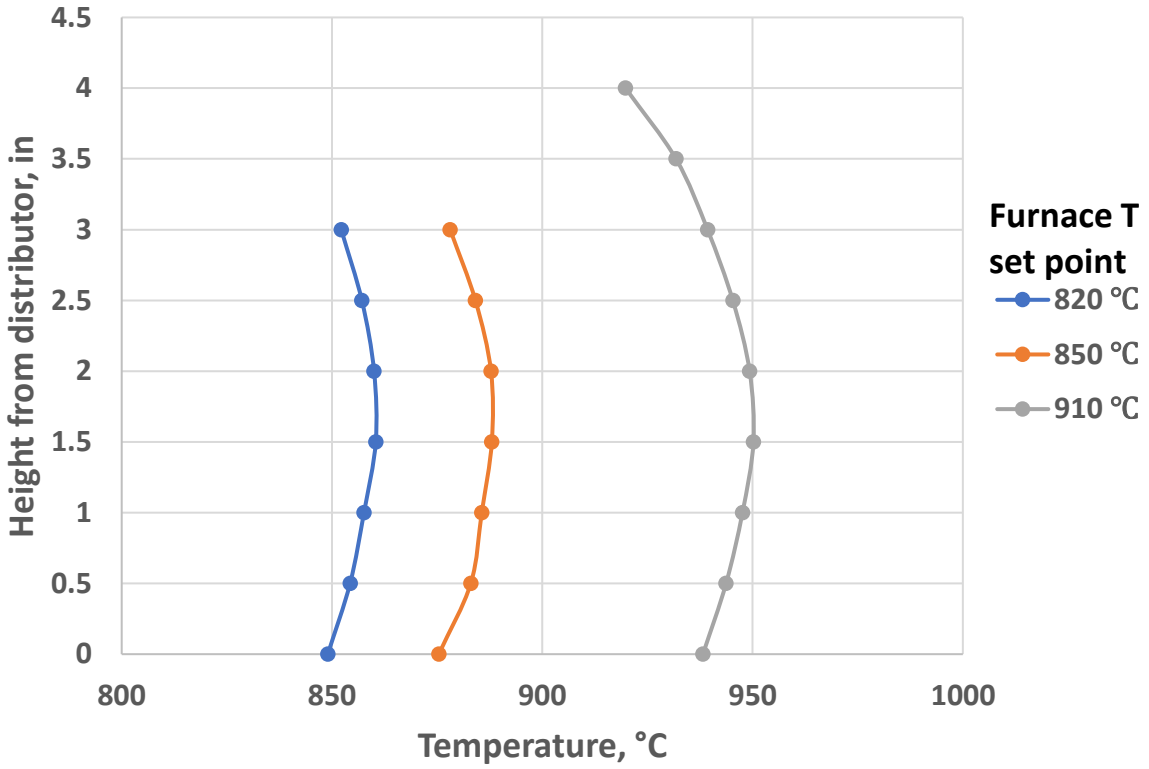

Figure 4. Reactor internal temperature profile at various setpoints.

To comply with the test conditions specified in

Table *1*, a sample loading of 27.53 grams was used. A mass spectrometer (MS) was utilized to monitor the flue gas composition. The MS was calibrated before and after each test. The material was heated to the test temperature under N_2 atmosphere, and then the reactor was pressurized to 7 bar(a). Once a stable temperature and pressure were reached, PCLC tests started.

Tests in

Table *1* were successfully conducted as planned, and samples were collected after each test. The results of the tests revealed that the oxygen carrier reacted vigorously when the gas was switched from N_2 to CH_4/CO_2. There was a significant CO_2 concentration peak immediately after the gas switch, as shown in Figure 1. It is worth noting that the CO_2 spike may have been attributed to both the reactions between the oxygen carrier and CH_4 and the presence of CO_2 in the gas stream.

*This project has received funding from the European Union's Horizon 2020 research and innovation programme under the Grant Agreement No **884418***

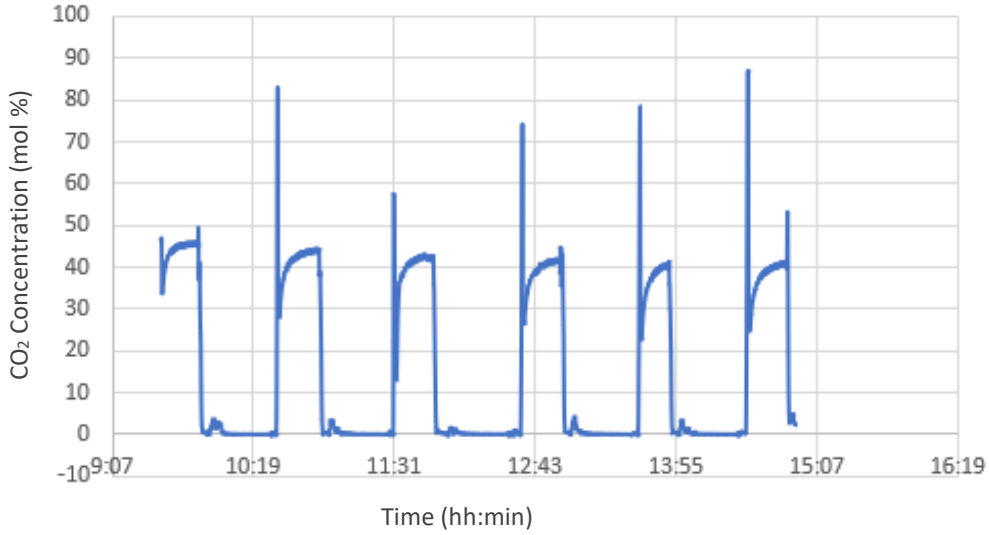

Figure 1. CO_2 concentration profiles during the oxygen carrier reduction (Test 7, first 6 cycles of a 10-cycle run).

In relation to CH_4, its concentration remained very low during the occurrence of the CO_2 spike. Only after the CO_2 spike decreased did CH_4 become detectable. This observation suggests that the initial CH_4 was completely consumed by the oxygen carrier, indicating a very fast reaction between CH_4 and the oxygen carrier. After consumption of the O_2 contained within the oxygen carrier, it would be expected that the measured concentration of CO_2 would be equivalent to the inlet CO_2 concentration (50 mol %), however as seen in Figure 5, the CO_2 concentration at the end of each cycle only reaches 40-45 mol %. This may be a result of reforming catalyzed by the reduced oxygen carrier. This hypothesis can be corroborated by the presence of mass numbers 2, 18 and 28 observed in the mass spectrometer, which could potentially correspond to H_2, H_2O and CO, respectively. Profiles associated to H_2 and CO appeared after the initial fast reaction stage. However, since these gases were not calibrated, their concentrations could not be determined.

As a consequence of the rapid reaction spikes at the start of each cycle, the reactor pressure experienced a rapid increase immediately after the gas switch. At the time of these tests, the reactor pressure was controlled manually, presenting significant challenges to maintain the target pressure of 7 bar(a). Once the reaction was over, the reactor pressure rapidly decreased, resulting in pronounced pressure fluctuations during the oxygen carrier reduction, as shown in Figure 2.

*This project has received funding from the European Union's Horizon 2020 research and innovation programme under the Grant Agreement No **884418***

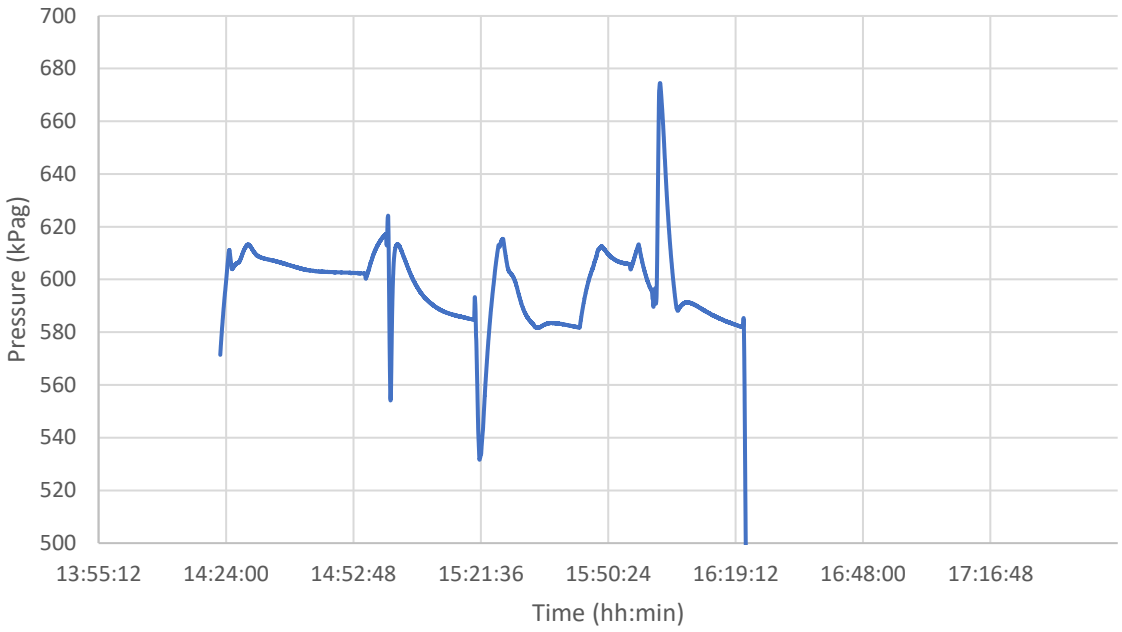

Figure 2. Reactor pressure during test (Test 6).

When the gas switched from N_2 to air, there was no detectable presence of O_2 for the first few minutes, which suggests that O_2 in air was completely consumed by the oxygen carrier for its oxidation. This phenomenon is illustrated in Figure 3, where the gas switched from N_2 to air at 15:58. It took approximately 4 minutes for O_2 to become detectable as it reacted with the oxygen carrier in the fluidized bed.

*This project has received funding from the European Union's Horizon 2020 research and innovation programme under the Grant Agreement No **884418***

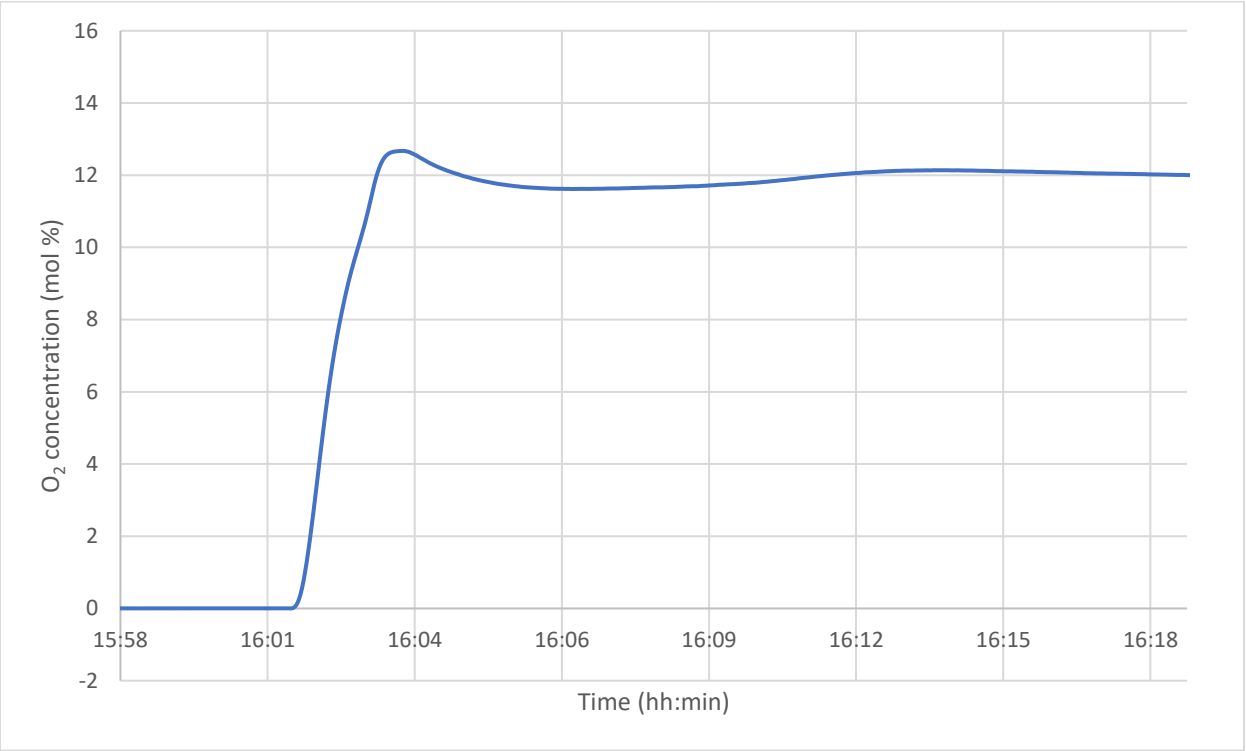

Figure 3. O_2 concentration during oxygen carrier oxidation (Test 7-CANMET).

Carbon deposition during oxygen carrier reduction was observed for a few tests. Particularly, Test #8 conducted at 925°C exhibited severe carbon deposition behavior, resulting in a significant increase in pressure differential across the reactor. In response, the duration of the oxygen carrier reduction step was reduced from 20 min to 15 min. As noted in

Table *1*, the oxidation period was extended to 60 min. This is because O_2 was first used to burn off the deposited carbon before it was used for oxygen carrier oxidation, resulting in a long period before O_2 concentration returned to normal levels.

Based on the pressure differential along the reactor, it is possible that carbon deposition also occurred during the lower temperature tests (850°C) with a reaction gas of CH_4/CO_2=1. However, tests with lower CH_4 concentration demonstrated less susceptibility to carbon deposition.

Carbon deposition could have arisen due to high CH_4 concentration and its reaction with the oxygen carrier, possibly proceeding to R2 in **Error! Reference source not found.**. The observed presence of H_2 and CO in the off-gas supports this hypothesis. However, it is also plausible that carbon deposition occurred due to the reaction between CH_4 and the reactor wall. To find this

*This project has received funding from the European Union's Horizon 2020 research and innovation programme under the Grant Agreement No **884418***

out, a test was carried out with an empty bed using a gas composition of CH_4/CO_2=1 at 925ºC, which led to carbon deposition. Therefore, it is probable that carbon deposition was mostly due to the reactions between CH_4 and the reactor wall.

The completion of this test campaign has highlighted several areas for future exploration in subsequent test work with the oxygen carrier to establish accurate reaction kinetics for PCL. The following should be considered in future tests:

- Calibration of mass spectrometers to measure H_2O and CO in the off-gas. However, it should be noted that using MS for flue gas analysis presents some difficulties. For example, CO overlaps with N_2 and CO_2, and quantifying H_2 becomes challenging in the presence of CH_4. Therefore, a based on the rapid reaction rates observed in previous tests.
- Automation of pressure control to reduce fluctuations observed during testing.
- Prevention of carbon deposition resulting from the reactions between CH_4 and the reactor wall.

6. Application of CO_2 partial pressure swings to the CASOH calcination stage and implications for heat management

CSIC has been investigating novel calcination strategies to accelerate the calcination of $CaCO_3$ in lime kilns and in a variety of calcium looping systems, CaL, including calcium-based sorption enhanced reforming processes and post-combustion CaL systems (10,11). The common objective of these calcination approaches is to reduce the heat requirements by lowering calcination temperatures through CO_2 partial pressure swings (by vacuum or by injection of steam). The understanding of the impact of fast partial pressure changes of CO_2 on the calcination rates of $CaCO_3$ dates back several decades. A seminal paper on calcination fundamentals (12) reported how the decrease in the partial pressure of CO_2 around a calcining stone (or a stone containing a core of $CaCO_3$) results in an initially fast calcination rate and a decrease in the temperature of the carbonated core limestone stones with a diameter over 1 cm. This section initially presents relevant experimental results carried out with the Ca-material planned for TRL7 testing within the WP2 of C⁴U, using particle sizes and reaction environments closer to what is expected in future CASOH processes. Additionally, a brief analysis is provided on the implications of these novel approaches to improve the heat management in the CASOH reaction stages. However, a more detailed analysis of process integration options is beyond the scope of this deliverable, as ongoing work is addressing this task in WP3. A comprehensive evaluation of full plant integration and cost analysis of the CASOH process incorporating the novel heat management strategies will be presented in Deliverable D3.4.

*This project has received funding from the European Union's Horizon 2020 research and innovation programme under the Grant Agreement No **884418***

5.1 Experimental testing of adiabatic cooling when applying vacuum around $CaCO_3$ calcining particles

In this subsection, we present the experimental evidence to proof the concept of a new calcination and heat management strategy (10) applied to packed bed calcium looping processes such as CASOH, resulting in the production of a pure stream of CO_2 during the calcination stage. The viability of the process relies on achieving adiabatic cooling in a preheated bed of $CaCO_3$-containing particles, by applying a vacuum swing to the bed of solids. The implications of this approach for the CASOH process are discussed in section 5.3 below and will be further explored in WP3. The experimental work to proof the concept has been carried in small-scale test facilities at CSIC-INCAR, which were previously used for other purposes (see for example a detailed description of the first rig shown in Figure 8 in (13).

Figure 8 provides an image of the experimental setup, where the key component is a fixed-bed reactor made of Inconel. The reactor has an internal diameter of 38 mm and a length of 0.92 m. To achieve pseudo-adiabatic conditions, the reactor is insulated with an 80 mm thick layer of rock wool, which serves as a thermal insulator. Both the reactor and the rock wool insulation are enclosed within a 14 kW refractory tubular furnace to compensate for heat losses to the surroundings. The tubular furnace allows for temperatures inside the reactor up to 900 ºC

To control the gas flow into the reactor, a set of mass flow controllers is employed for gases such as CO_2, N_2, and air. These controllers operate effectively within a range of 0 to 30 LN/min. The gases are preheated using a system consisting of two thermal belts, providing power outputs of 450 W and 780 W respectively, raising the temperature of the incoming gases to approximately 500ºC. To measure the longitudinal temperature profiles inside the reactor, an inconel sheath containing 14 K-type thermocouples distributed axially is used. At the reactor outlet, a silica gel bed is used to effectively remove the water vapor that is generated during operation.

Continuous monitoring of gas concentrations, based on a dry basis, is conducted using SICK GM800 analyzers. An infrared module measures CO_2 in two ranges of 0-10% vol. and 0-100% vol. The O_2 concentration is measured using a paramagnetic analyzer within a range of 0-21%. Data acquisition is carried out using an Agilent 34972A unit, which allows for the continuous recording of temperatures and gas concentrations at the reactor outlet.

*This project has received funding from the European Union's Horizon 2020 research and innovation programme under the Grant Agreement No **884418***

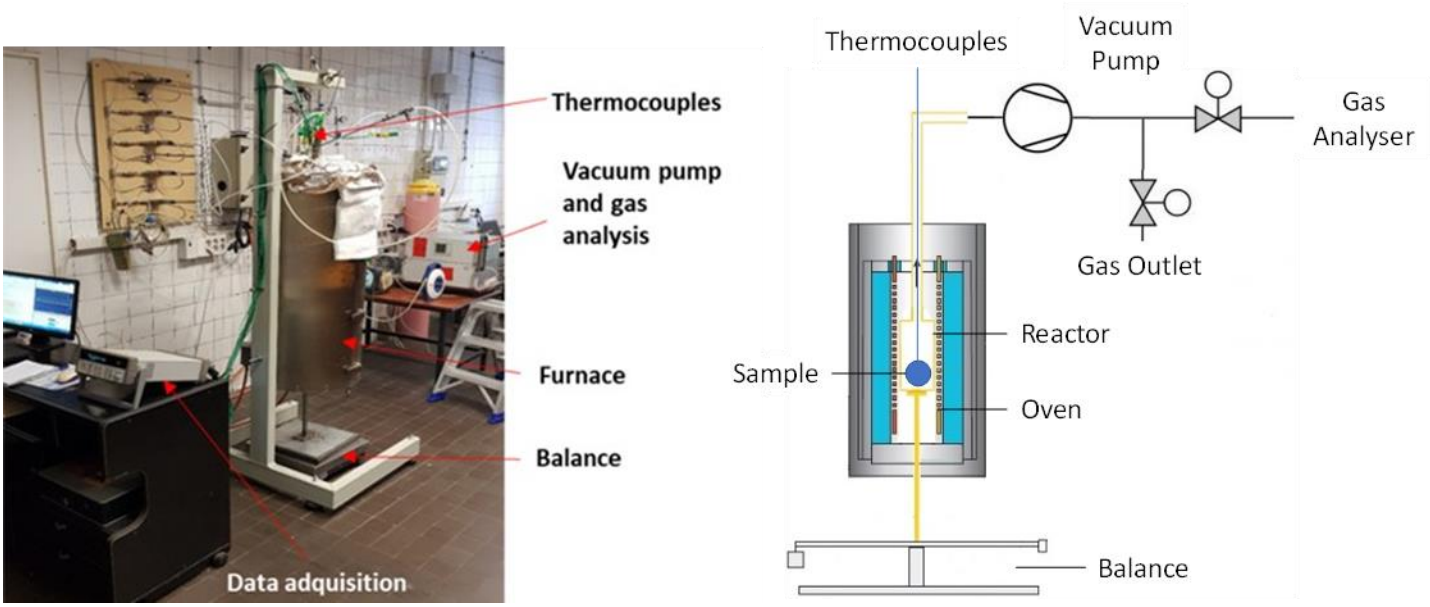

Figure 8: Experimental set up at CSIC-INCAR used to conduct the initial vacuum calcination tests using large limestone particles (d_p=20 mm)

Different experiments were conducted for the study of the calcination of $CaCO_3$ particles when applying vacuum. Initially, a single limestone stone with a diameter of 20 mm and a mass of 5.4 g was used, which was placed inside the furnace with a thermocouple to measure the surface temperature ($T_{s,out}$). Additionally, another thermocouple was embedded inside the stone, serving the dual purpose of holding it in place and measuring the temperature at the centre of the solid ($T_{s,in}$). Finally, a third thermocouple positioned a few centimeters from the particle was used to monitor the gas temperature (T_{gas}) during the experiment. Furthermore, a small flow of 1 NL/min of N_2 was circulated to detect variations in CO_2 concentration at the reactor outlet, and successive pressure changes between 1 and 0.1 bar were applied. Figure 9 shows the evolution of gas and solid temperatures, as well as the outlet gas concentration during the pressure swings applied to the reactor. Initially, the reactor was heated at atmospheric pressure until a temperature of 860ºC was achieved by feeding pure CO_2 to prevent limestone calcination. Once a uniform temperature was achieved in the experimental setup, a vacuum of up to 0.1 bar was applied by operating a pump connected downstream of the reactor. As can be seen in Figure 9, the application of vacuum dramatically decreased the temperature inside the particle ($T_{s,int}$) to 810ºC as a result of the rapid calcination of $CaCO_3$, which is highly favoured under these operating conditions. Additionally, the temperature on the surface of the solid ($T_{s,out}$) also decreased, although to a lesser extent due to the significant thermal inertia present in the reactor (T_{sgas} remained constant throughout the experiment).

Regarding the gas concentration at the reactor exit, a peak in CO_2 concentration was observed due to the rapid calcination after the pressure swing, although this CO_2 concentration quickly

*This project has received funding from the European Union's Horizon 2020 research and innovation programme under the Grant Agreement No **884418***

dropped as the temperature in the particle decreased. In this experiment, once a certain stability in both temperature and CO_2 concentration was reached, the pump was stopped to restore the atmospheric pressure in the reactor. From that moment onwards, the calcination of $CaCO_3$ abruptly ceased, and the solid temperature rapidly increased due to the heat transfer received from the gas phase at 860ºC.

The pressure swing was repeated following a sequence of ten vacuum-heating cycles in order to progressively calcine the particle of limestone. During the initial cycles, the observed trends remained consistent, and during the vacuum stage, the solid cooled rapidly to temperatures close to 810ºC, resulting in a gas with nearly 4% vol. of CO_2. However, when the pressure was raised to atmospheric conditions, the calcination (and then the CO_2 production) ceased, and the temperature inside the solid increased to 835ºC in only 3 minutes. As the calcium-based particle approached the complete calcination, the temperature drop observed during the vacuum stages gradually diminished as expected, resulting in a reduced generation of CO_2. Finally, after 10 cycles, the particle achieved complete calcination, and the measured temperatures in the solid reached the gas phase temperature (i.e., 860ºC).

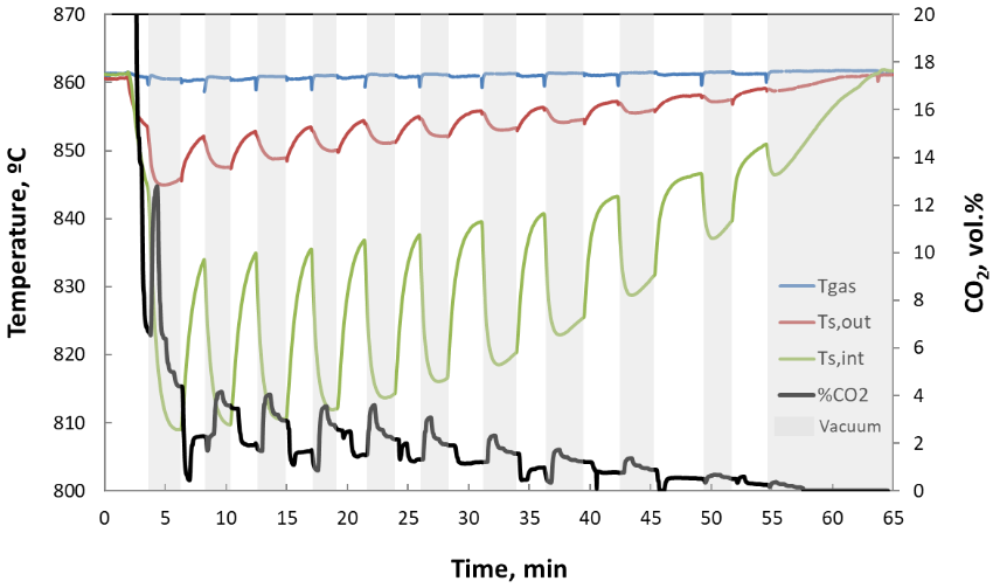

Figure 9. Evolution of temperatures and product gas concentration during successive vacuum calcination cycles using a single particle of limestone (d_p=20 mm).

In subsequent experiments to test vacuum effects on calcination, a small batch of 377 g of limestone (dp of 20 mm) was positioned in the interior of the reactor (showed in Figure 8) on a bed of inert solids, as indicated in Figure 10. Moreover, several K-thermocouples were introduced in the bed to monitor the temperatures when imposing a fast vacuum swing on the preheated bed of solids. Two thermocouples were used to measure the temperature of the gas phase at the beginning of the Ca-based solids bed (T_{gas}, L=57 cm) and near the reactor outlet

*This project has received funding from the European Union's Horizon 2020 research and innovation programme under the Grant Agreement No **884418***

at the top of the bed (T_{gas}, L=30 cm). Additionally, two thermocouples were placed to measure the evolution of the temperature inside and on the surface of a limestone particle located at the top of the bed (Ts, L=25 cm). Figure 10 shows the evolution of solid and gas temperatures during successive vacuum calcination cycles starting with the bed of solids previously heated in an atmosphere of 100% CO_2 to temperatures above 850ºC to prevent premature calcination of $CaCO_3$ in the limestone. The thermocouples measuring the temperatures of the gas phase initially showed a variation of 35ºC across the bed (from 885ºC at L=57 cm to 850ºC at L=30 cm) as a result of the limitations of the furnace to maintain a uniform temperature along the reactor.

Once stable temperatures were achieved in the experimental setup, a vacuum of up to 0.1 bar was applied by operating a pump connected downstream of the reactor. In this experiment, no gas flow was circulated during the cycles, so it was not possible to measure the CO_2 concentration in the product gas during the calcination stages. However, a flow meter was placed at the reactor outlet to monitor the flow of CO_2 resulting from the calcination of $CaCO_3$. As can be seen in Figure 10, the application of vacuum dramatically decreased the temperature inside the solids ($T_{s,int}$) from 875ºC to 845ºC after 1 minute of operation in the first cycle. As happened in the previous experiment, the temperature on the surface of the solid ($T_{s,out}$) also decreased but to a lesser extent (from 875 to 865ºC) due to the thermal inertia in the reactor imposed by the furnace. The significantly larger amount of limestone present in this experiment resulted in a high energy consumption during the vacuum calcination stages to decompose the $CaCO_3$, causing adiabatic cooling in the bed and thus a decrease in gas phase temperatures. During the vacuum calcination stage, an outlet flow of approximately 5 NL/min of CO_2 was recorded. After 1 minute of operation, the pump was stopped to increase the pressure of the reactor up to atmospheric conditions. As expected, the calcination of $CaCO_3$ ceased, stopping the production of CO_2, whereas the temperature of the reactor increased due to the heat transferred from the furnace. After 5 minutes at atmospheric pressure, the temperature of gas and solid achieved their initial conditions. The pressure swing was repeated during 23 cycles until the total calcination of the $CaCO_3$ present in the bed was achieved. As the calcination cycles progressed, the temperature drop inside the particle during the vacuum stages was decreasing until less than 10ºC in the final cycles. Meanwhile, the flow rate of CO_2 produced was also decreasing 5 Nl/min measured in the first cycles to 3 Nl/min between cycles 5-10 and less than 2 Nl/min in the last 3 cycles.

*This project has received funding from the European Union's Horizon 2020 research and innovation programme under the Grant Agreement No **884418***

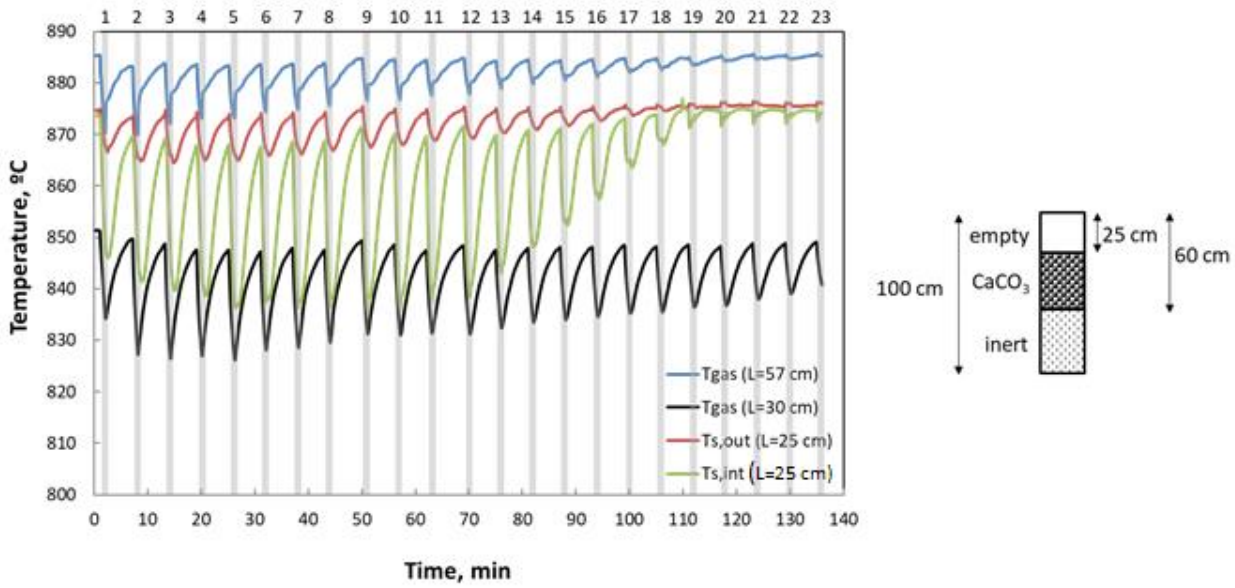

Figure 10.. Evolution of solid and gas temperatures during successive vacuum calcination cycles using a bed of limestone (d_p=20 mm) placed on inert material.

In an attempt to obtain results closer to ideal adiabatic conditions during the adiabatic cooling induced by vacuums swing on highly cycled materials in calcium looping processes (i.e. with a substantial fraction of sintered CaO as indicated by molar Ca conversions below 4% plotted in Figure 11), a bed of $CaCO_3$-containing solids (185 g) were arranged in a packed bed surrounded by insulating material, as shown in Figure 11. This bed was then covered by a welded metallic vessel and placed inside the oven of Figure 8 to allow similar vacuum swing tests as described above. However, to better reproduce the expected phenomena in continuously operated calcium looping systems, a highly sintered CaO-based material (overburnt commercial lime supplied by Carmeuse, consisting of CaO particles of 4 mm diameter obtained in an oven at 870°C) was used in these tests. As can be seen in Figure 11, the insulation of the solids bed allowed a precise monitoring of temperature drops within the bed when subjected to vacuum swings between 0.05 and 1.3 bara).

*This project has received funding from the European Union's Horizon 2020 research and innovation programme under the Grant Agreement No **884418***

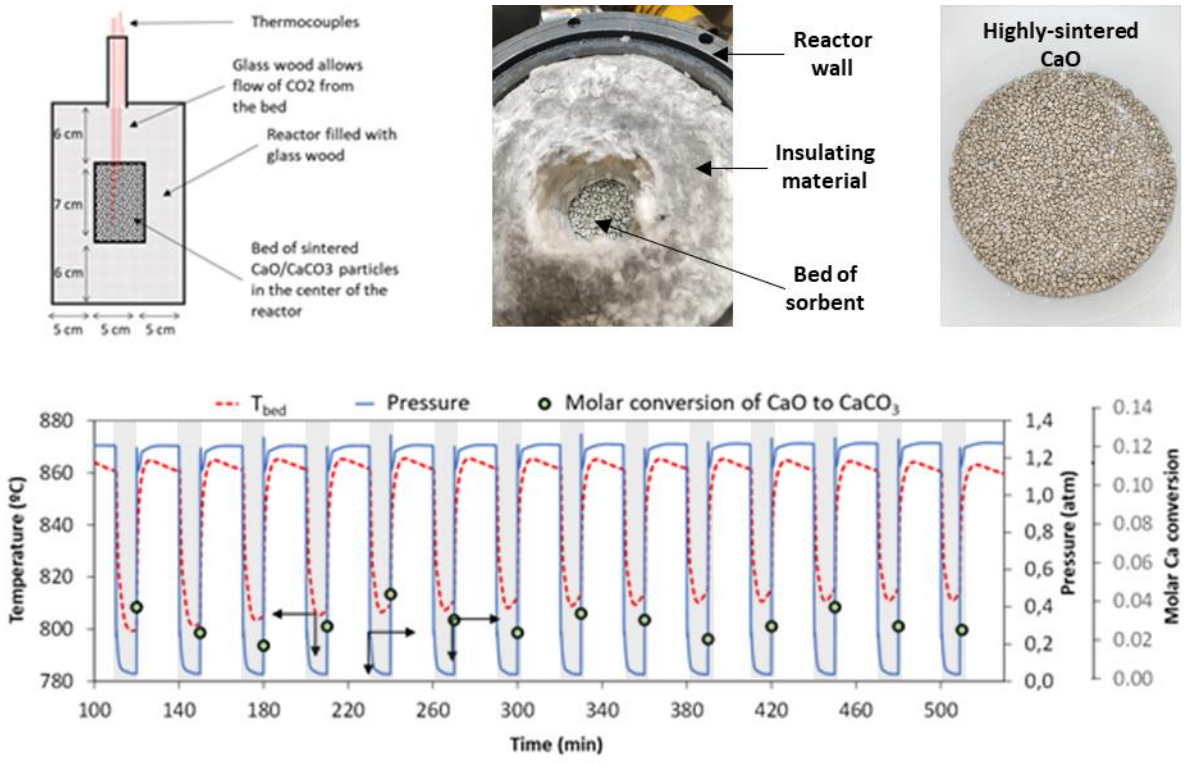

Figure 11. Experimental results for vacuum swing calcination followed by carbonation over 14 cycles using a CaO material with low maximum carbonation capacity (about 3.4% molar conversion in average), plotting 14 consecutive cycles involving vacuum and heating steps. Dotted lines represent the temperature evolution in the centre of the bed (left axis) when a vacuum swing (solid line, right axis in atm) is applied. The white dots (second scale on the left-hand side) represent the evolution of the average increase or decrease in calcium carbonate conversions during the cyclic operation.

These results provide initial evidence of the feasibility of operating a calcium looping system that incorporates the vacuum swing calcination principle. The reversibility of both the carbonation/calcination conversions and the temperature profiles observed in the bed of particles is remarkable, considering the low CO_2 carrying capacity characteristic of these highly sintered CaO-materials. Fast calcination under vacuum is observed even at temperatures as low as 800ºC. These particles have a low content of $CaCO_3$ (0.034 is the average carbonation conversion or carbonate content in this experiment, as marked by the green dots of Figure 11 in the molar Ca conversion scale on the right). Due to the low initial carbonate content, the material is fully calcined after a single vacuum-calcination step and the cooling due to calcination is halted at about 800ºC (calcination time 10 min). To initiate a new heating and vacuum cycle, pure CO_2 was fed into the reactor to carbonate the material (carbonation time 15 min) back to its maximum CO_2 carrying capacity of 0.034 (molar Ca conversion), which is consistent with the modest but highly reversible CaO materials in the

*This project has received funding from the European Union's Horizon 2020 research and innovation programme under the Grant Agreement No **884418***

CASOH reactors. Since the particles are too small to track individually their temperatures in this set up, a bed of 185g of CaO particles was used, surrounded by a 5 cm thick layer of low conductivity silica-wool material This setup allows for the detection of temperature drops when the vacuum stage of the cycle is applied. The application of vacuum swing from 1.2 atm to 0.05 atm is represented by the solid line (pressure scale on the right-hand side). The temperature measured within the bed is represented by a dashed line (temperature scale on the left-hand axis). In this case, the maximum temperature achieved in the bed during the heating step is 860ºC, while the minimum approaches 800ºC. The temperature swing recorded in the bed of solids in this experiment was about 60ºC, whereas the adiabatic temperature linked to the average measured changes in carbonation or calcinations conversions of 0.034 should be 124ºC. The observed discrepancy can be attributed to the conduction of heat through the metallic thermocouple wall, as the insulating layer of silica wool impeded the fast heat transfer from the oven to the centre of the bed. The analysis of the solids at the end of the experiment confirmed the average carbonate conversion of 0.034, which aligns well with the average molar Ca conversions (between carbonation and calcination) plotted in Figure 11, determined by the recorded weight differences during the test. The previous experimental results, along with the modelling carried out to interpret them as described in section 5.3, demonstrate that within reasonable heating times (5-20 minutes), it is possible to transfer the necessary energy (50-150 kJ/kg) to solids containing $CaCO_3$ to bring them back to an average temperature of 800-900ºC, necessary to re-initiate a new vacuum cycle step, where temperatures will drop between 30-200ºC (causing a decrease in molar $CaCO_3$ content between 0.01 and 0.07) in the solids. The calcination rates under vacuum step are sufficiently fast to complete an incremental calcination molar conversion of 0.01 and 0.07 in just 5-20 minutes of the vacuum stage, at vacuum pressures between 0.05-0.5 atm.

Finally, a series of vacuum swing calcination test were carried out using the same $CaCO_3$ material selected for TRL7 testing of the CASOH process. This material is a limestone supplied by Carmeuse/Techforlime, which possesses suitable mechanical properties for packed bed operations and "standard" reactivity properties in terms of CO_2 carrying capacities (i.e. standard decay curve), carbonation and calcination rates. Expanding upon the strategy described in previous paragraphs, a new reactor setup was built at CSIC-INCAR to investigate a range of pressure swing high-temperature looping processes using the CASOH materials with the aim of achieving close-to-adiabatic curves during vacuum swings.

The experimental setup consisted of a fixed bed reactor with an inner diameter of 50 mm and a total length of 1.35 m. The reactor was made of 310 stainless steel. An electric heater with a power capacity of 3.5 kW is assembled at the reactor inlet to preheat the reactant gases. This preheater could operate at a maximum temperature of 1000ºC, with a minimum flow rate of 1.6 Nm^3/h. The test rig also included several mass flow controllers to feed mixtures of air, N_2 and CO_2 up to a maximum total flowrate of 50 Nl/min.

*This project has received funding from the European Union's Horizon 2020 research and innovation programme under the Grant Agreement No **884418***

To compensate heat loss, the reactor was enclosed within a ceramic oven with a height of 1.2 meters. The oven, with a diameter of 125 mm and a power output of 5 kW, featured three distinct heating zones. This configuration allowed rather uniform temperature profiles along the reactor. A 2-meter long Inconel 600 multipoint thermocouple (D=8 mm) equipped with 10 measuring points was used to monitor the evolution of the axial temperature during the experiments. The setup also included a non-dispersive infrared analyser to quantify CO_2 and a paramagnetic analyzer for measuring O_2. Finally, a pump was connected to the reactor outlet to carry out the vacuum operation.

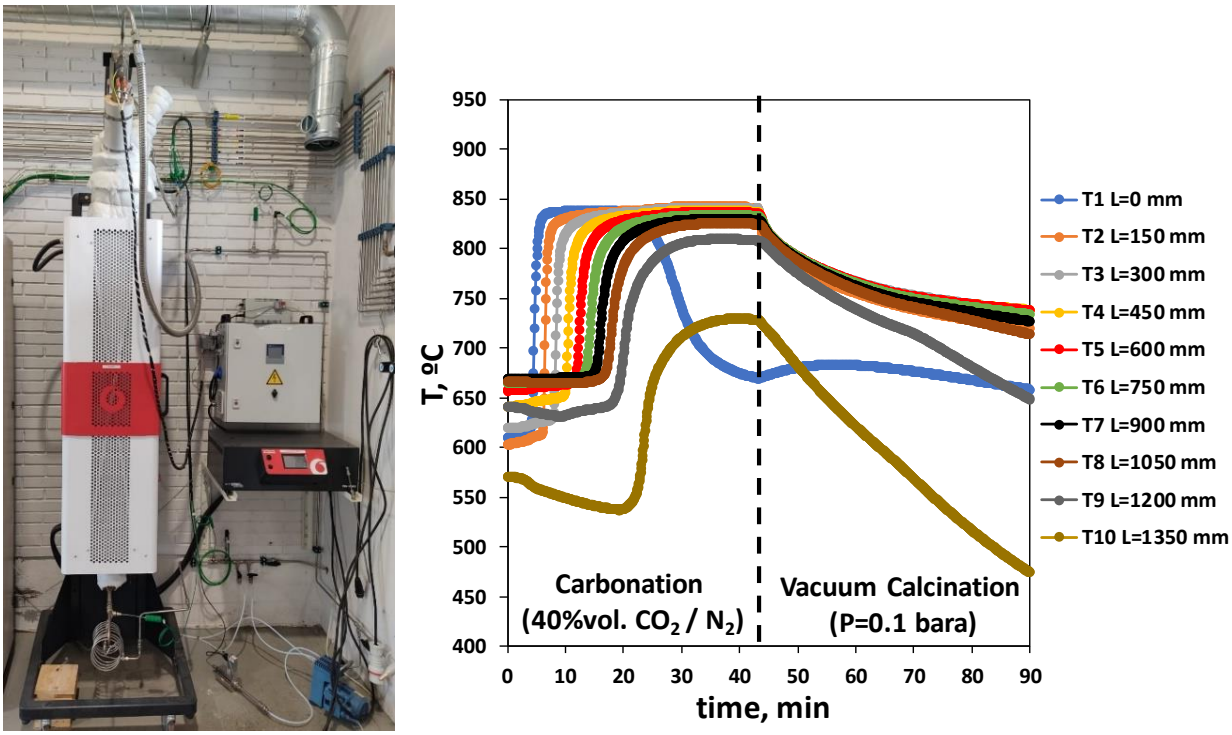

Figure 12. Left: Experimental set up at CSIC-INCAR used to conduct vacuum calcination test of the limestone chosen for TRL7 testing. Right: experimental temperature profiles.

For the experiment represented in Figure 12, a batch of 2 kg of limestone (from the 3 tonne batch provided by Carmeuse for TRL7 experiments in WP2) was first loaded into the bed and calcined overnight in air at 800ºC. Once the material had been calcined, a feed gas containing 40% CO_2 (which can be considered an approximation of the composition of CO_2 in the CASOH carbonator reactor when accounting for the CO_2 produced during WGS in the CASOH stage) caused sharp T profiles as shown in Figure 12 (right). The temperature profiles observed were consistent with the expected values in an adiabatic reactor, considering the exothermic enthalpy of carbonation and the high CO_2 carrying capacity of this material during the first carbonation cycle. As the carbonation reaction caused the solids bed to reach temperatures

*This project has received funding from the European Union's Horizon 2020 research and innovation programme under the Grant Agreement No **884418***

approaching 850°C, a fast swing to vacuum conditions was possible at about 42 minutes of the experiment. As can be seen in the results shown in Figure 12 (right), the temperature profiles dropped sharply all over the bed, which aligns with previous observations in Figures 9-11. These results confirm that when the pressure swing is imposed by the application of a vacuum pressure, all particles in the bed undergo a pressure swing in partial pressure of CO_2 at the same time (assuming pressure transmission occurs at the speed of sound, which can be considered instantaneous for the time scales involved in these experiments). Similar to previous tests conducted with individual particles and smaller batches of $CaCO_3$ containing materials, the rate of calcination decreases quickly after the first few minutes.

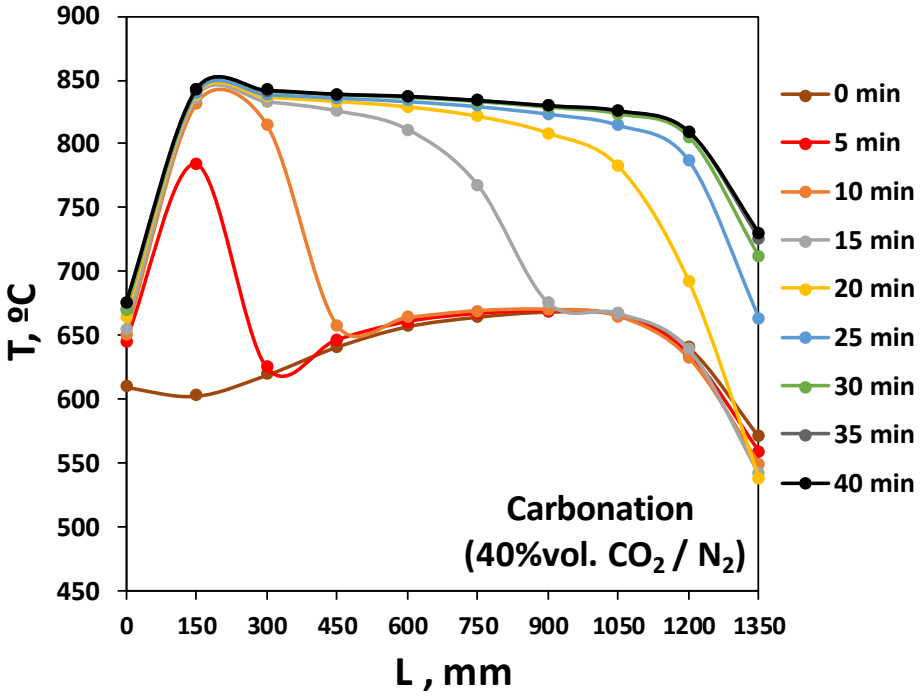

Figure 13. Left: evolution with time of the temperature profiles during carbonation of an active bed of CaO in the set up of Figure 12.

Figure 13 provides a more detailed representation of the temperature profile evolution in the bed of CaO particles when feeding a flow of CO_2/N_2 (40%vol CO_2) preheated to 650°C? to a bed of solids preheated to just an optimum temperature (average about 600 °C) to initiate CASOH reactions. The figure clearly demonstrates the pseudo-adiabatic behaviour of the reactor, with

*This project has received funding from the European Union's Horizon 2020 research and innovation programme under the Grant Agreement No **884418***

the top 300 mm of the bed (closest to the inlet of gases) reaching the maximum temperature in less than 10 minutes, which is consistent with the evolution of a neat carbonation reaction front originating from the top of the bed and progressing downwards. These results are fully consistent with observations reported in the literature (7,5) in different set ups when investigating the CASOH reactions at TRL4-3. However, as mentioned above, the experimental set up of Figure 12 allows for a fast vacuum swing to be applied to the bed, enabling the extraction of pure CO_2 with the vacuum pump, and the recording of the evolution with time of the axial temperature profiles in the bed as the vacuum pressure decreases from 1 atm to 0.1 atm. The corresponding results are presented in Figure 14.

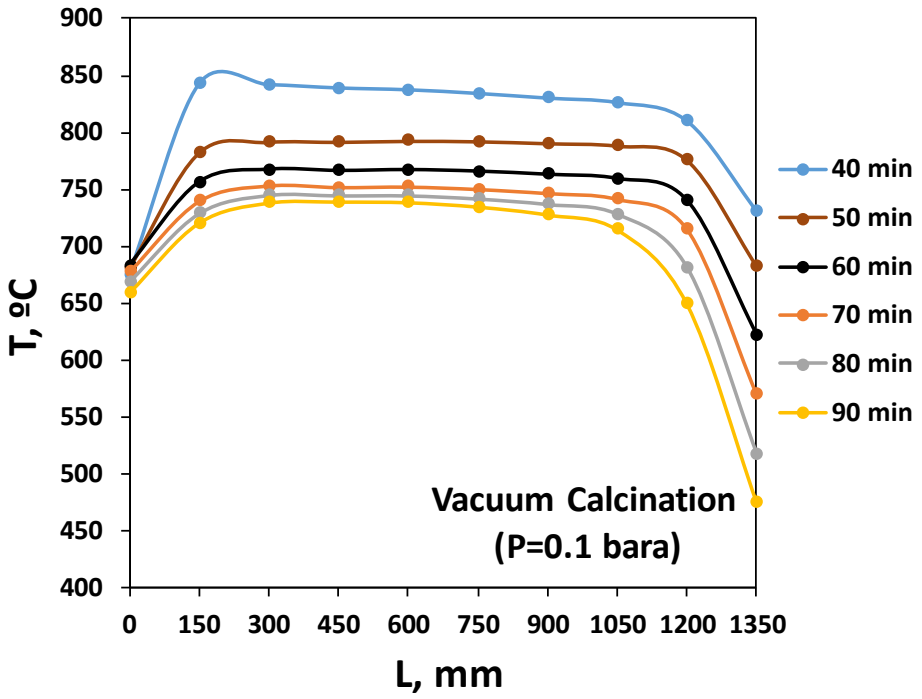

Figure 14. Left: Experimental set up at CSIC-INCAR used to conduct vacuum calcination test of the limestone chosen for TRL7 testing. Right: experimental temperature profiles.

Figure 14 confirms previous findings regarding the impact of a vacuum swing step on a preheated bed of $CaCO_3$ (in this case heated mainly by the carbonation reaction carried out in a previous step as shown in Figure 13). Apart from the two positions in the bed closest to the inlet (left-hand side) and outlet (1350 mm, right-hand side), there is a clear temperature plateau that undergoes an almost simultaneous adiabatic cooling in the whole length of the bed. The rate of the cooling is faster at the beginning, in line with the higher temperatures and the steep slope of the equilibrium calcination curve of CO_2 on CaO. Indeed, the temperature measured in the bed during this experiment closely matches with the equilibrium temperature

*This project has received funding from the European Union's Horizon 2020 research and innovation programme under the Grant Agreement No **884418***

of CO_2 on CaO at the pressure of CO_2 measured at any point in the time of the first 90 minutes of this experiment. This observation facilitates the application of existing reactor models for the CASOH process to the enhanced versions of the CASOH process that emerge from these experiments and that are discussed in section 5.3 below.

5.2 Experimental testing of adiabatic cooling when applying steam around $CaCO_3$ calcining particles

As mentioned above, another method of inducing partial pressure swings of CO_2 around calcining particles of $CaCO_3$ is by introducing steam into the calcination atmosphere. From a fundamental perspective, when considering the phenomena occurring at microscopic level and/or small particle level during calcination under differential and well controlled conditions, the calcination rates should not be affected by the nature of the inert gas that dilutes the CO_2 (14) in the atmosphere of calcination. In practical terms, the calcination rates for particles relevant to CASOH applications (typically with dp>3mm) are mainly governed by heat transfer resistances from the external surface of the particle towards the core rich in $CaCO_3$, as well as by the mass transfer of CO_2 towards the exterior of the particles (12). Furthermore, when considering the operation of packed bed reactors as those expected in the CASOH process, the generation of sharp reaction and heat transfer fronts in the bed is a common occurrence, similar to other gas-solid reaction systems using packed beds to carry out fast exothermic or endothermic reactions. In these conditions, the overall heat and mass transfer between stationary reacting solids and the gases that pass through the bed is strongly affected by gas properties and fluid-dynamic conditions related to the gas passage through the bed. Consequently, in order to experimentally investigate the impact of a partial pressure swing of CO_2 by steam addition to a packed bed of $CaCO_3$ containing solids, dedicated experiments were carried out using the same test facility at CSIC-ICB used for CASOH reactions reported in D2.3 and in a recent publication (5). The test facility includes an electrically heated fixed bed reactor (with an inner diameter of 18 mm), and has been equipped with a capability to feed steam to a preheated bed of $CaCO_3$ containing particles. Figure 15 shows an image of the experimental rig (Left) and a scheme of gas flow and main elements in the reactor (Right) during steam assisted calcination test.

The reactor is heated up by an electric wire resistance (1.2 kW electric power), and covered by an insulation layer to minimize heat losses. It is instrumented with a series of thermocouples immersed in the reactor, that allow measuring and recording the evolution of bed temperature while the calcination reaction is taking place. The rig includes gas mass flow controllers (N_2 and CO_2) and a liquid mass flow controller. To introduce the vaporized water, the system has been equipped with a secondary reactor and a dedicated furnace. At the main reactor exit

*This project has received funding from the European Union's Horizon 2020 research and innovation programme under the Grant Agreement No **884418***

there is a condenser, and an aliquot of product gas stream is sent for analysis to a micro-GC (Varian CP-4900). Bed temperature is controlled by the thermocouple located in the bottom part of the reactor, that is the last portion of bed facing the reaction front. As will be seen below, thanks to this arrangement, the power input to the reactor does not react during several minutes to the temperature variations due to reaction (i.e. the adiabatic cooling expected when introducing steam to the preheated $CaCO_3$ solids).

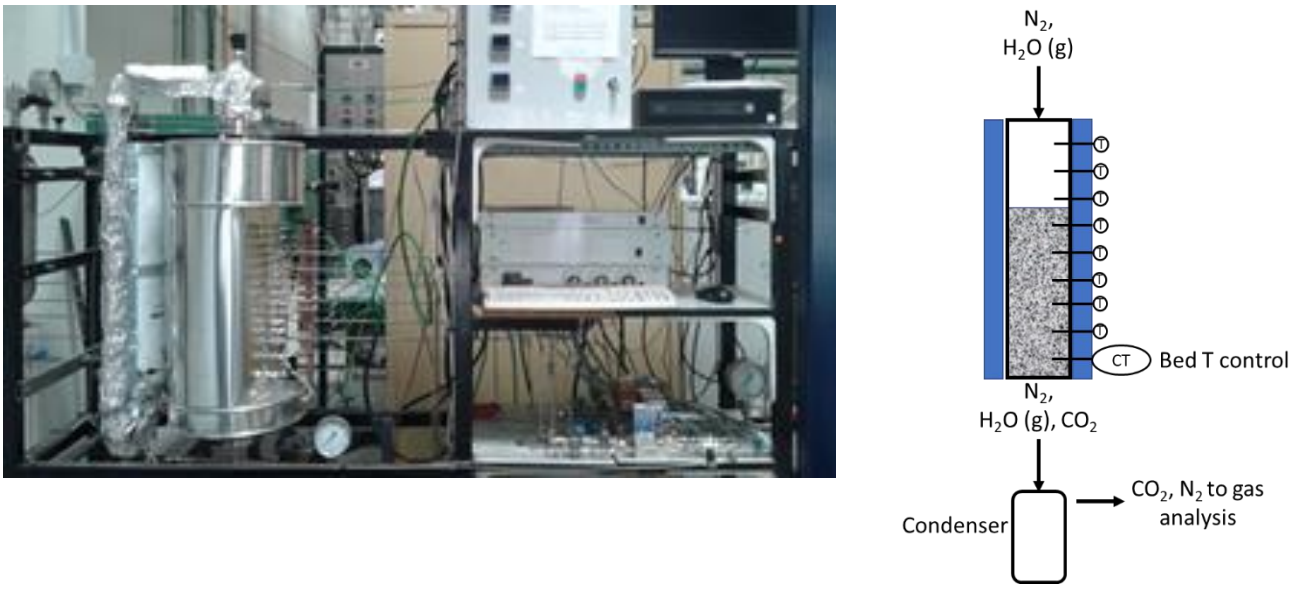

Figure 15. Left) Image of the experimental rig. Right) Scheme with gas flow and main elements in the reactor.

Therefore, any temperature change measured in the bed following the switch to steam can be attributed to the calcination reaction (as long as this is sufficiently fast). The limestone used for the calcination tests was supplied by Carmeuse and corresponds to the same material that will be utilized in the TRL-7 plant. For the experiments carried out in the TRL-3 reactor, the limestone was sieved and particles within the range of 1-2 mm were selected. A total of 70 g of limestone was loaded into the reactor, resulting in a bed length of 15 cm with 6 thermocouples positioned within the bed to measure temperature.

The experimental procedure begins with a heating-up period in 100 % vol. CO_2, raising the temperature to approximately 900 °C while preventing $CaCO_3$ decomposition. The control thermocouple was set at 880 °C. At a specific point in time, the gas entering the reactor was switched to a mixture concentrated in steam. A small percentage of N_2 (up to 20%vol) was fed into the system to serve as a carrier for the steam, and to determine the carbon balance in the gas at reactor outlet by gas analysis. In these experiments, due to the non-adiabatic behavior

*This project has received funding from the European Union's Horizon 2020 research and innovation programme under the Grant Agreement No **884418***

of the small rig, the electric heating wire was maintained on, and the electric power input to the oven was monitored, so to facilitate interpretation of fast cooling/heating observed in the bed. It is important to note that the thermocouple used to control the oven was positioned at the bottom part of the bed, which means that the power input to the reactor was unaltered during the steam assisted calcination test, even when the initial bed slices were cooling down due to calcination (see below). This arrangement enabled the observation of the adiabatic cooling due to $CaCO_3$ calcination under the fast-partial pressure swing in CO_2 experienced by the particles located at the top of the bed when switching to the steam/N_2 feed gas. Once the cooling phenomenon reached the control thermocouple, the control system of the oven activated the power input to the system, indicating the completion of the test. As shown below, several multicycle experiments were performed, with a N_2 flow of 3 l/h and a steam flow of 6.2, 8.7 and 12 l/h (all in normal conditions).

As an illustrative example of experimental results, Figure 16 shows bed temperature evolution with time from the moment when steam/N_2 mass flow controllers were opened. Two periods can be distinguished in the figure (labeled 1 and 2). During the first period, a transient phase occurred due to gas dispersion issues in the rig (i.e. departure from ideal plug flow behavior). As a result, the N_2/steam flow was not well developed and an incipient calcination took place only in the two first slices in bed. Since the reactor atmosphere was mainly CO_2 from the heating-up period, the gas entering the initial bed slice was very close to equilibrium conditions, and only a very slow temperature decrease was observed. Then, a well-developed steam/N_2 flow arrived to the bed surface, leading to the detection of a fast cooling front moving from the upper part of the bed (2.5 cm) towards the bottom. The right side of Figure 16 provides a closer view of the adiabatic cooling caused by $CaCO_3$ calcination in the steam/N_2 flow. During this adiabatic cooling, the temperature measured in the control thermocouple (15 cm) was largely unaltered, indicating that the electric wire did not increase the power input to the reactor. Consequently, calcination occurred due to the sensible heat stored in bed of $CaCO_3$ of solids and adiabatic cooling took place to drive the endothermic calcination reaction imposed by the change in partial pressure of CO_2 by the steam injection. Figure 16 reveals that calcination progressed gradually along the bed, with a gradual temperature drop observed across all thermocouples. Such drop temperature was less pronounced in the bottom part of the bed, as the gas entering these slices contained a certain % vol. CO_2 that must be close to the equilibrium of CO_2 on CaO at the temperature of the solids in that slice.

During the calcination test, CO_2 concentration was measured at reactor exit after steam condensation, and the experimental results were introduced in the Figure 16. As it can be observed, an 80 % vol. CO_2 in the wet gas was measured, and therefore the CO_2 in gas stream corresponded to equilibrium concentration at the highest temperature measured in bed (Temperature from thermocouple at 12.5 cm).

*This project has received funding from the European Union's Horizon 2020 research and innovation programme under the Grant Agreement No **884418***

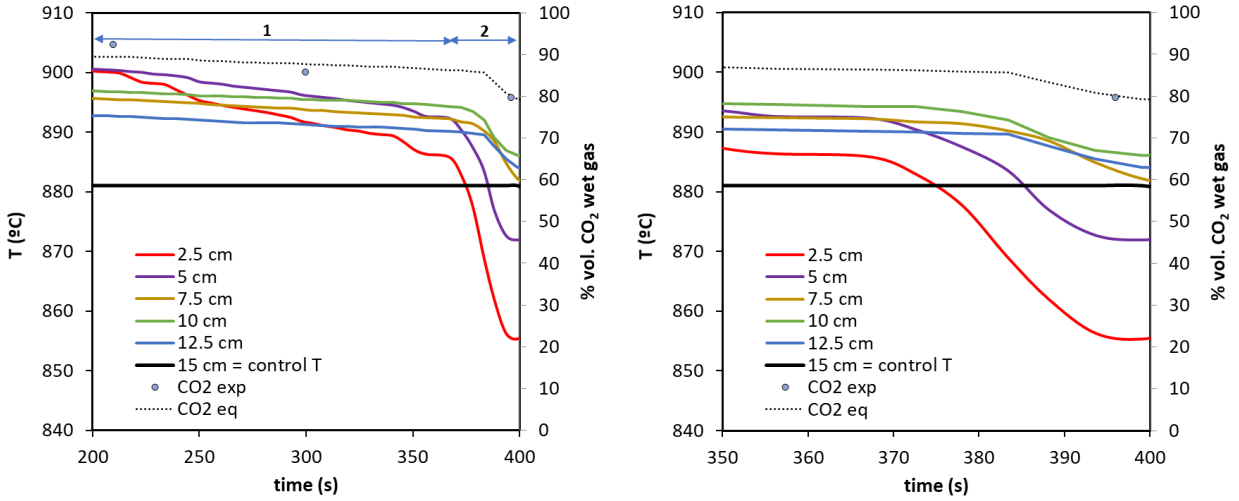

Figure 16. Left) Bed temperature evolution with time for a test performed with a sweeping N_2/steam flow of 0.05 m/s at reactor inlet. Right) Zoom to the experiment from the left Figure.

In the absence of a comprehensive mathematical model capable of quantitatively explaining all the main phenomena observed in this particular experimental set up, these results can be interpreted qualitatively, as shown in Figure 17. This figure represents the progress of the calcination front within bed, according to the adiabatic cooling phenomena induced by steam injection. When the N_2/steam flow reaches bed surface, $CaCO_3$ calcination takes, resulting in the cooling of the bed slice while simultaneously generating CO_2. Calcination occurs until pCO_1 reaches the equilibrium concentration at the cooled slice temperature (T_1). It is important to note that this differs from situation described in section 5.1, where the vacuum swing imposes a "simultaneous" pressure swing on all particles in the bed (i.e. assuming that the speed of transmission of the pressure swing from the vacuum pump to the particles is close to the speed of sound). In contrast, when steam is used as sweeping gas to induce the partial pressure swing, the limited gas velocity of the steam in these experiments (between 0.03 to 0.07 m/s to provide a gas residence time comparable to that expected in larger TRL reactors) governs the rate at which the particles experience the pressure swing in different parts of the bed. Consequently,, the gas entering the second slice (L_2) will contain N_2/steam/p_1CO_2, and the calcination front will progress if CO_2 partial pressure at slice 2 inlet (L_2) is lower than the equilibrium CO_2 partial pressure at slice 2 temperature (T_2). In other words, calcination will occur whenever $p_nCO_2 < p_{n+1}CO_{2(eq)}$, and therefore, CO_2 at reactor exit will reach equilibrium with the temperature of the hottest point in bed.

*This project has received funding from the European Union's Horizon 2020 research and innovation programme under the Grant Agreement No **884418***

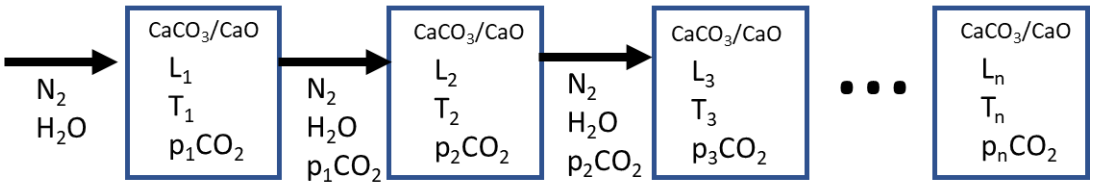

Figure 17. Schematic representation of calcination front progress observed in Figures 16 and 18.

The amount of CO_2 present in the gas exiting each slice will be determined by the equilibrium (assuming the calcination reaction rate is not limited by other controlling factors such as the particle size). Consequently, the gas flowrate used for the sweeping will have an impact on the reactor calcination rate, and on the progression of the calcination front. In this way, with higher sweeping gas flowrates the calcination on every slice may not reach the equilibrium, resulting in a more gradual progress of the calcination front along the reactor. In contrast, with lower sweeping gas flows, the gas may leave the slice reaching equilibrium, causing the calcination of the following slice to delay until the previous bed slice is almost completely calcined.

According to the schematic representation in Figure 17, a higher steam flow would result in a larger number of moles of $CaCO_3$ being calcined until equilibrium is reached. As a result, the cooling phenomena would progress faster in bed. Figure 18 shows experimental data at two different N_2/steam flows: figure on the left with a linear gas velocity at bed inlet of 0.036 m/s, and the figure on the right with a linear gas velocity at bed inlet of 0.064 m/s. Observing the Figure on the left, the temperature drop in the first thermocouple is relatively fast. However, for the rest of the thermocouples, the temperature drop occurs in less extent, and there is almost no temperature drop for the thermocouple at 7.5 cm or deeper in bed. In this case, after just 35s, the calcination front only reached the second thermocouple immersed in bed. In contrast, the Figure on the right shows a fast drop in temperature in all thermocouples, and the calcination front reached the control thermocouple at 15 cm in approximately 20 s.

*This project has received funding from the European Union's Horizon 2020 research and innovation programme under the Grant Agreement No **884418***

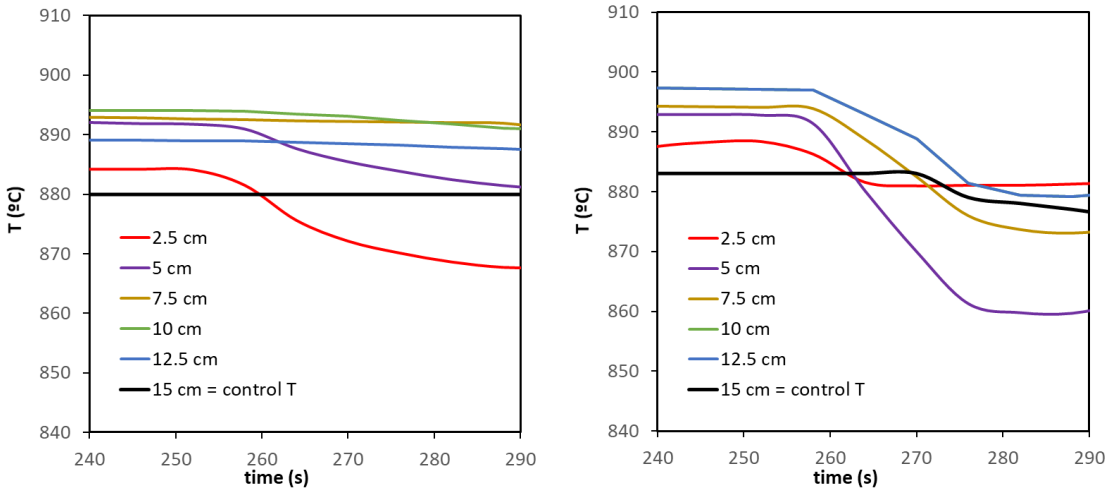

Figure 18. Left) Bed temperature evolution with time for a test performed with a sweeping N_2/steam flow of 0.036 m/s at reactor inlet. Right) Bed temperature evolution with time for a test performed with a sweeping N_2/steam flow of 0.064 m/s at reactor inlet.

Figure 19 represents normalized temperature drop with time from the moment when the developed flow steam/N_2 reaches the bed surface for three different steam/N_2 linear gas velocities evaluated. As it can be observed in the Figure, a higher N_2/steam flow leads to a significantly faster cooling due to calcination. For instance, a temperature drop of 33 ºC is observed in approximately 15 s, while a ΔT of -25 in 27 s has been observed for the experiment with a N_2/steam flow of 0.05 m/s, and 15 ºC in 30 s for the experiment performed at 0.036 m/s. Gas analysis has been facilitated the calculation of the average calcination rate within the bed for the three sweeping gas flows tested. The results indicate that 1.14 mol CO_2/m^2s was calcined with a sweeping flow of 0.036 m/s, while 1.53 mol CO_2/m^2s was calcined with a sweeping flow of 0.050 m/s, and 1.92 mol CO_2/m^2s was calcined for the highest sweeping flow tested (0.064 m/s).

*This project has received funding from the European Union's Horizon 2020 research and innovation programme under the Grant Agreement No **884418***

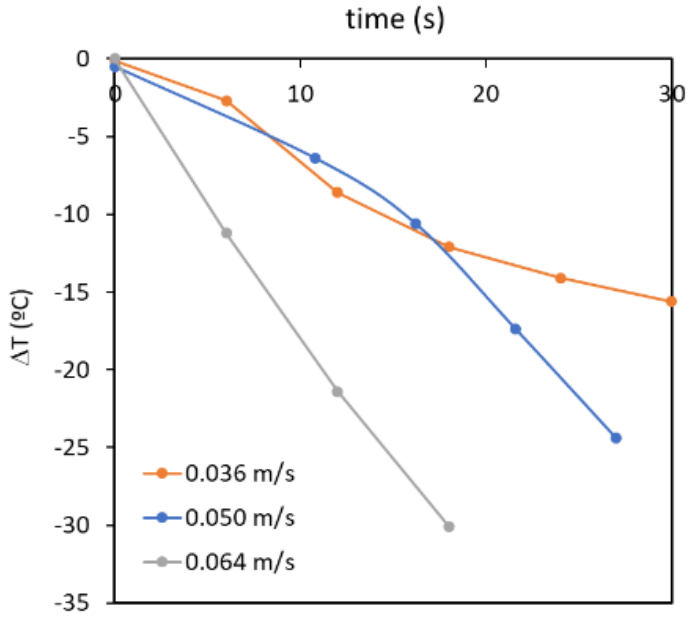

Figure 19. ΔT vs time comparison for three N_2/steam sweeping gas velocities at reactor inlet (at 900 ºC).

Finally, it must be noted that for a given N_2/steam flow, the progression of the calcination front will also depend on the amount of $CaCO_3$ present in the bed (and its distribution along the length of the bed). Consequently, in a bed with lower $CaCO_3$ content, the progression of the calcination front will be faster, and calcination will occur progressively along a longer bed length. In this case, as the same batch of solids has been consecutively calcined/carbonated during the experimental campaign, the amount of $CaCO_3$ in bed will have decreased progressively with the number of cycles performed. This can be observed in Figure 20, that represents two calcination tests conducted with a N_2/steam sweep flow of 0.050 m/s. The Figure on the left corresponds to the third carbonation-calcination cycle, while the Figure on the right represents the sixth cycle. As can be seen in the Figure on the Left, a fast-adiabatic cooling is observed for the initials slices in the bed, with a ΔT of approximately 50 ºC in the first thermocouple immersed in the bed of solids, and 27 ºC in the following slice. In contrast, a ΔT of only 22 ºC is observed for the first slice in the calcination test represented on Figure on the Right, followed by a 30 ºC ΔT in the second bed slice.

*This project has received funding from the European Union's Horizon 2020 research and innovation programme under the Grant Agreement No **884418***

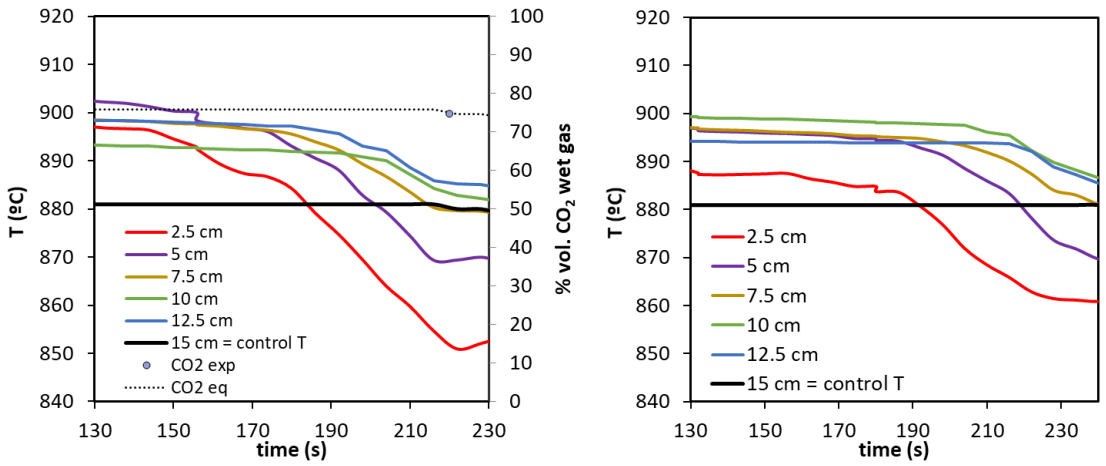

Figure 20. Bed temperature evolution with time for a test performed with a sweeping N_2/steam flow of 0.050 m/s at reactor inlet, Left) cycle 3. Right) cycle 6.

Overall, the previous experimental results in sections 5.1 and 5.2 represent a first proof of concept on the possibility to substantially improve the heat management of the CASOH process by exploiting the phenomena of "adiabatic cooling" when a bed containing $CaCO_3$ preheated to calcination temperatures is submitted to a fast swing of partial pressure of CO_2. Such partial pressure swing can be induced by either applying vacuum or introducing steam into the bed, resulting in a rapid progression of calcination. Consequently, a highly pure CO_2 stream is generated (pure CO_2 in the case of vacuum swings, and CO_2 easy to purify by condensation of steam in the second case) at the exit of the reaction stage undergoing calcination. The fact that sensitive heat (at temperatures above800ºC allowing very fast calcination rates of $CaCO_3$) can be used as the main energy source to drive calcination reactions (instead of chemical energy from a fuel gas as represented in the Regeneration stage of Figure 1) may have important implications for the CASOH process, as described in the next section.

*This project has received funding from the European Union's Horizon 2020 research and innovation programme under the Grant Agreement No **884418***

5.3 CASOH reactor performance improvements when applying CO_2 vacuum swings during calcination

This section describes a set of simulations carried out with the current version of the CASOH reactor model when implementing partial pressure swings during the calcination stage, consistent with those discussed in section 5.2. The objective of this section is therefore to better understand the implications in the operation of the CASOH reaction stages at larger scale when implementing operating options involving fast CO_2 partial pressure swings during the calcination stage. The model used in this section has been described in detail in Deliverable D2.3 and in two recent publications (5, 15). It has been validated so far with experimental data from all the reaction stages and bed compositions of the CASOH process, investigated at TRL4 and TRL3 as described in (5, 7). Unfortunately, the validation with experimental results at TRL7 is still pending, due to the delay in the commissioning of the CASOH pilot. Despite the current lack of validation of the model under vacuum swing conditions, there is sufficient information in the previous sections and in the literature on calcination kinetics to adapt the model to the new conditions created around the particles when altering their gas environment.

The dynamic reactor model used to carry out these simulations takes into account the following assumptions: plug flow pattern with axial mass and thermal dispersion, negligible radial gradients, ideal gas behavior, adiabatic conditions, absence of temperature and concentration gradients at the inter-particle level, uniform particle size and void fraction and perfect mixing of the Ca- and Cu-based solids in the bed. Furthermore, the model assumes the characteristics of the commercial Cu- and Ca-based materials utilized in the CASOH process demonstration at the TRL7 pilot plant. This includes the incorporation of kinetic parameters obtained through thermogravimetric analyses, as reported in Deliverable 2.3 and in the recent publication by Grasa et al.(5). The carbonation of CaO-based particles can be described using a homogeneous reaction model that incorporates an effectiveness factor to account for internal diffusional resistances. With respect to the calcination stage, the evolution of the solid conversion can be well represented by means of a shrinking core model (SCM) (6), including an effectiveness factor of 0.04 to tackle internal diffusion limitations in the solid during calcination. Regarding the redox reactions in the Cu-based material, a Shrinking Core Model (SCM) assuming cylindrical geometry and chemical reaction control without internal diffusion is employed to describe both reduction and oxidation reactions.

The reactor model includes a set of partial differential and algebraic equations, which have been solved using MATLAB programming. A spatial discretization method on the reactor has been implemented using finite differences. This approach transforms the model into an initial-value problem governed by a nonlinear system of ordinary differential equations (ODEs) containing unknown functions of time t. To solve the stiff ODE system resulting from the

*This project has received funding from the European Union's Horizon 2020 research and innovation programme under the Grant Agreement No **884418***

discretization, a variable order and variable step size MATLAB algorithm have been utilized.
A reference case was examined to demonstrate the feasibility of the new CASOH operation strategy, which incorporates CO_2 partial pressure swing calcination by applying vacuum combined with steam injection. This process scheme favours the fast calcination of $CaCO_3$ with a reduced consumption of steam, as will be discussed in more detail when considering process integration works ongoing in WP3. For this study a typical composition of BFG consisting of 23% vol. CO, 21% vol. CO_2, 3% vol. H_2, and 53% vol. N_2 was assumed. A total inlet flow to the CASOH process of 4 kmol/s of BFG was considered, and a reactor size with a length of 12 m and an inner diameter of 6 m was chosen (i.e. a L/D ratio of 2), which falls in the range reported for large-scale packed-bed reactors (16). Assuming the characteristics of the Ca- and Cu-based materials listed in Table 2, about one sixth of the inlet BFG (i.e. 0.67 kmol/s) can be upgraded and decarbonized via the CASOH stage in one reactor in approximately 20 min. The CASOH stage was carried out at 10 bar with an initial temperature in the bed of 720 °C. A flow of 0.3 kmol/s of steam allowed a S/CO molar ratio of 2 in the feed, which was introduced into the reactor preheated at 720 °C.

Table 2. Solid bed properties for the reference case.

Conditions	**Value**
Reactor Length, m	12
Reactor Diameter, m	6
Bed density, kg/m^3	1500
Cu-based material present in the bed, wt.%	20
Ca-based material present in the bed, wt.%	80
CaO active content in the Ca-based material, wt.%	4.5
CuO active content in the Cu-based material, wt.%	14

The initial conditions of the solids bed at 720 °C and 10 bar ensured from the very beginning that the CO contained in the BFG reacted with steam to produce H_2 and CO_2 via WGS, and the

*This project has received funding from the European Union's Horizon 2020 research and innovation programme under the Grant Agreement No **884418***

CO_2 was rapidly removed from the gas phase through the carbonation of CaO. As a result of that, a flow of 0.71 kmol/s of product gas was obtained, containing 23.5 vol% H_2 in 53.5 vol.% N_2 with only 1.6 and 2% vol.% of CO and CO_2, respectively (on a wet basis), as can be seen in Figure 21.

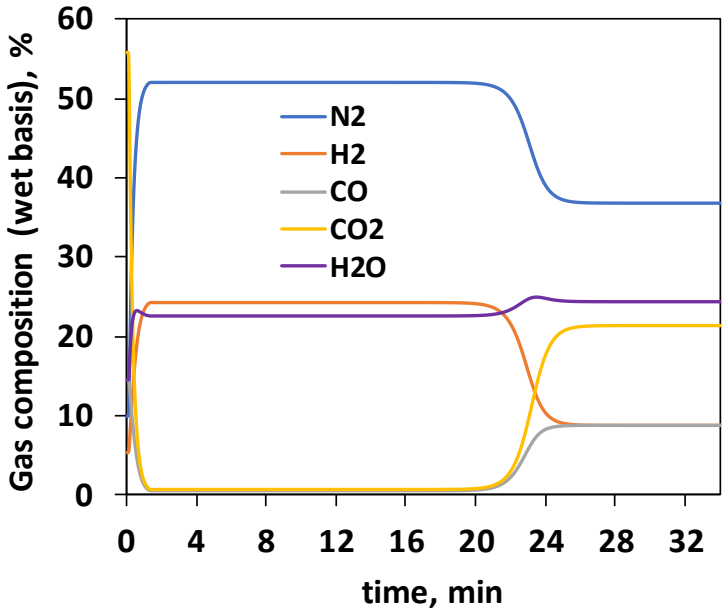

Figure 21. Dynamic profile of gas composition (%.vol) inside the packed-bed reactor during CASOH Stage.

As can be seen in Figure 22, due to the high concentration of CO_2 generated via the WGS of BFG, the carbonation of CaO was highly favoured, and a rapid increase in the temperature profile was observed, until a maximum value near 850 °C was achieved. The carbonation front advanced very fast along the packed bed leaving behind totally carbonated solids (see Figure 23) at a heat plateau of 850 °C. After a little more than 20 min of operation, the temperature front approaches the final section of the reactor, whereas a small fraction of the bed closer to the reactor inlet is left at temperatures between 720 and 850°C. At that time, the bed approached almost total carbonation and the CASOH stage finished. Extending more time this stage would drastically reduce hydrogen production and the CO_2 capture, since the packed bed would act as a WGS reactor (see Figure 21).

*This project has received funding from the European Union's Horizon 2020 research and innovation programme under the Grant Agreement No **884418***

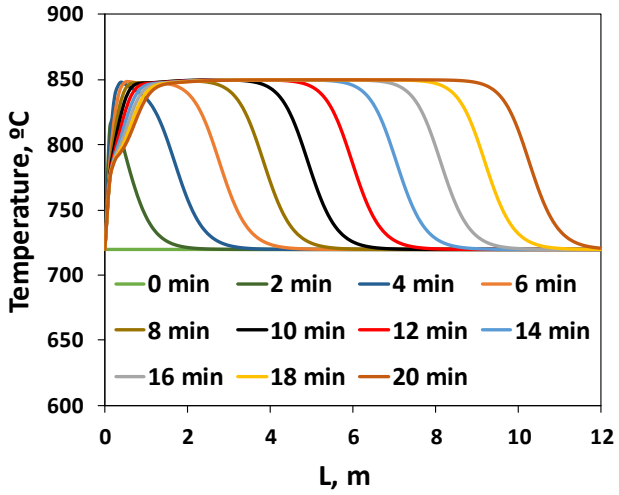

Figure 22. Dynamic profile of temperature (ºC) inside the packed-bed reactor during CASOH Stage.

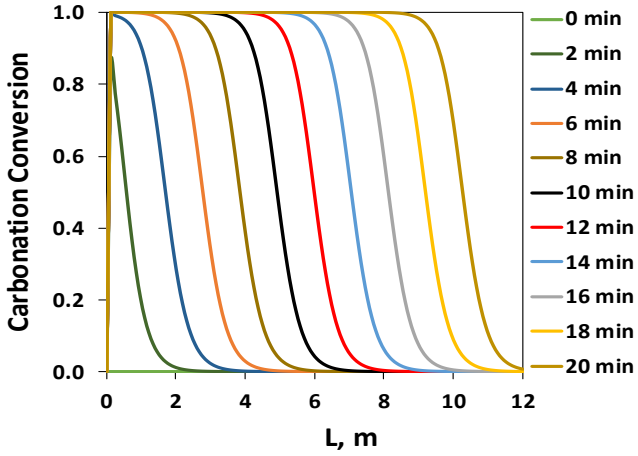

Figure 23. Dynamic profile of solids conversion inside the packed-bed reactor during CASOH Stage.

As shown in Figure 22, after the CASOH stage, the heat generated during the carbonation of the active CaO present in the bed remained stored in the solids at a temperature of about 850 ºC. Such a high temperature in the carbonated solids allows the application of a moderate vacuum until 0.5 bar, in combination with the injection of steam at a temperature of 720 ºC, to cause a rapid CO_2 partial pressure swing in the reactor, that favoured a fast calcination of $CaCO_3$. To this end, a flowrate of 0.18 kmol/s of steam was fed into the packed bed to complete the calcination stage in approximately 20 min, as the previous CASOH. Steam was introduced in counter current flow by the part of the bed left at higher temperature to favour the total calcination of the carbonated solids from the very beginning.

*This project has received funding from the European Union's Horizon 2020 research and innovation programme under the Grant Agreement No **884418***

As can be seen in Figure 24, as the $CaCO_3$ calcination proceeded, the temperature of the bed gradually decreased due to the heat consumed in such endothermic reaction, consistent with the experimental observations of section 5.2. As can be seen in Figure 25 a product gas of 0.47 kmol/s wad obtained, containing an average concentration of 60%vol and 40 %vol of CO_2 and steam, respectively. Consequently, almost pure CO_2 can be obtained after steam condensation downstream of the reactor.

At the end of the calcination stage, the solids were left almost totally calcined (except in the small fraction at the bottom of the bed affected by the inlet temperature of the BFG during the CASOH stage). What is especially important is to realize that most of the heat accumulated in the reactor during the carbonation reactions taking place during the previous CASOH stage was consumed for calcination thanks to the partial pressure swings forced on the solids by applying vacuum and feeding steam. However, note that the bed of solids was left at slightly high temperature compared to the initial temperature of the CASOH (i.e. a fraction of the bed with a heat plateau at 735 °C instead of the initial temperature of 720 °C). This was due to the additional heat generated during the WGS reaction of the CO contained in the BFG.

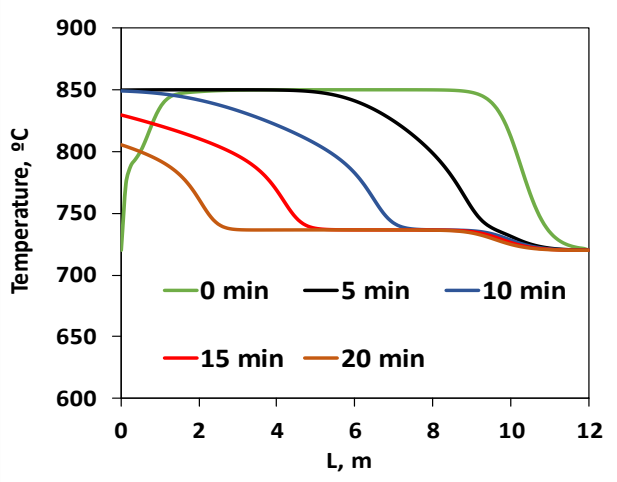

Figure 24. Bed temperature evolution along the packed-bed reactor by applying CO_2 partial pressure swing calcination.

*This project has received funding from the European Union's Horizon 2020 research and innovation programme under the Grant Agreement No **884418***

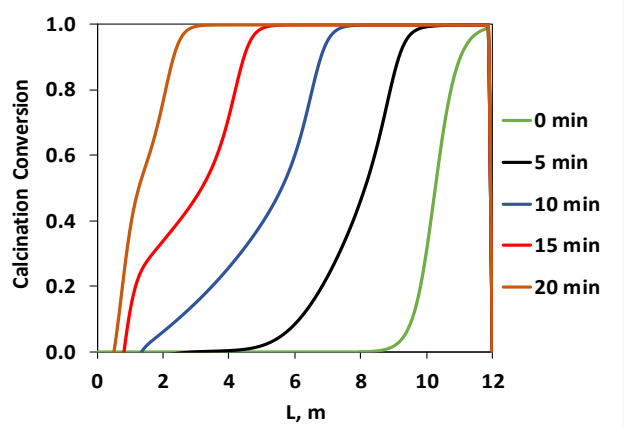

Figure 25. Calcination conversion along the packed-bed reactor.

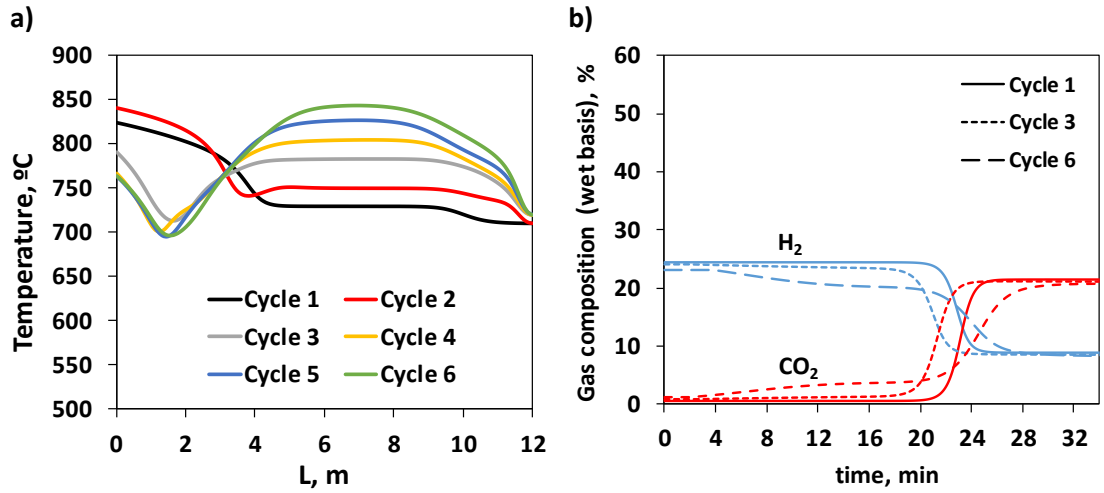

Figure 26. a) Bed temperature (ºC) evolution along the packed bed reactor after each CASOH cycle b) Evolution of the product gas composition during the CASOH stage.

Despite the accumulation of the energy released by WGS as sensitive heat in the bed of solids, the operation at 10 bar during the CASOH stage allows for successive CASOH+calcination stages to be carried out, without significantly reducing for the first few cycles the production of H_2 and the CO_2 capture efficiency during the CASOH stages (see Figure 26). However, after 6 CASOH/calcination cycles, the bed temperature reaches an average value in the central region of about845 ºC that will limit H_2 yields the CO_2 capture efficiency if an additional CASOH stage is carried out (See Figure 26).

At this point, a heat removal stage must be introduced to remove the excess heat stored in the solids. In the absence of other endothermic reactions to be used for this purpose (i.e. reforming reactions such as those reviewed for Ca-Cu systems in ref (3)) the heat removal can be carried

*This project has received funding from the European Union's Horizon 2020 research and innovation programme under the Grant Agreement No **884418***

out by flowing through the bed a N_2 gas recycle, with the heat recovered from the recirculated N_2 used to produce high or intermediate-pressure steam for power generation, or to produce the steam required for the CASOH process and/or to preheat gaseous feedstock. Details of such process integration scheme will be discussed in Deliverable 3.4 in the coming months. However, the simulations of the reactors discussed in previous paragraphs confirm the potential for improved heat-management strategies of the CASOH processes by exploiting the experimental observations in section 5.2 regarding calcination-enhanced reaction stages using vacuum swing and/or steam addition to the calcining bed of solids.

7. Conclusions

This deliverable includes two different contributions by CANMET/NRCAN and CSIC, to investigate alternative reactor schemes that both have potential capability to decarbonise fuel off-gases from steel-making processes (such as Coke Oven Gas, with the main carbon source in the form of CH_4, or Blast Furnace Gases, with the main carbon source in the form of CO and CO_2). As other high-temperature looping cycles, both approaches claim inherently higher energy efficiencies when exploiting the reversibility of Cu-based chemical looping combustion and calcium looping reactions at high temperatures. In both cases, experimental progress has been achieved in a range of TRL3-4 installations as shown in this deliverable, testing new materials and heat management strategies.

The experimental work and proof of concept carried out CANMET/NRCAN provides a first proof of the viability of a new fluidised bed-based chemical looping combustion at high pressures and temperatures (up to 30 bar and 950ºC), using fuel gases containing CH_4. The results of the tests in the new experimental facility at CANMET revealed that the oxygen carrier reacted vigorously with the Cu-containing oxygen carrier when the gas was switched from N_2 to CH_4/CO_2. There was a significant CO_2 concentration peak immediately after the gas switch. When the gas switched from N_2 to air, there was no detectable presence of O_2 for the first few minutes, which suggests that O_2 in air was completely consumed by the oxygen carrier for its oxidation. Carbon deposition during oxygen carrier reduction was observed for a few tests (particularly, severe in a test at 925ºC), resulting in a significant increase in pressure differential across the reactor. To eliminate the carbon, the oxidation period was extended, with O_2 from air first used to burn off the deposited carbon before it was used for oxygen carrier oxidation. Future process simulation work should assess the implications of the such carbon leakage during the oxidation stage.

In a different front, CSIC has reported experimental evidence on a new heat management strategy for the CASOH process, that relies on the enhanced calcination rates (and associated adiabatic cooling of the calcining solids) when a fast swing in partial pressure of CO_2 is caused on the solids resulting from a sorption enhanced water gas shift reaction of Blast Furnace

*This project has received funding from the European Union's Horizon 2020 research and innovation programme under the Grant Agreement No **884418***

Gases with CaO (i.e. a CASOH reaction stage) to produce H_2. It has been experimentally demonstrated in various experimental set ups, and with different materials (individual small stones of limestone of 20 mm diameter, small beds of sintered CaO partially carbonated and the actual $CaCO_3$ solids chosen for TRL7 testing of the CASOH process), that reducing vacuum pressure (down to 0.1 atm) allows for fast drops of temperature of the calcining solids to temperature as low as 720ºC. More moderate vacuum pressure swings demand for higher temperatures of heating of the carbonated solids and/or higher number of vacuum cycles to achieve complete calcination, as the drop in temperature of the solids will be limited by the moderate rate of calcination at conditions close to the equilibrium temperature imposed by the vacuum pressure. The observations of adiabatic cooling and accelerated calcination rates are confirmed also in experiments where the partial pressure swing is caused by injection of steam to the bed of preheated $CaCO_3$ solids. In this case, the evolution of the temperature profiles with time during calcination strongly depends on the velocity of the injected steam in the bed. On the other hand, model predictions using the current version of the model for the CASOH reactors, reveal that it is possible to exploit the adiabatic cooling phenomena to improve the heat management of the CASOH process, because the energy released during the carbonation of CaO during a CASOH reaction stage (while producing H_2 from BFG) can be largely re-used for calcination of $CaCO_3$ (and therefore for the regeneration of CaO for a new CASOH reaction stage). Therefore, it can be concluded that calcination-enhanced processes by partial pressure swings will lead to higher H_2 yields (or cold-gas efficiencies) than initial versions of the CASOH process, and should become a priority for development and further experimental testing at TRL7 in the C⁴U project.

8. Bibliography / References

1. C⁴U Project. Advanced Carbon Capture for the Steel Industry integrated in CCUS Clusters. [Internet]. (2020) Available from: https://c4u-project.eu/
2. Abanades, J.C, Arias, B., Lyngfelt, A., Mattisson, T., Wiley, D.E, Li, H., et al. Emerging CO_2 capture systems. *Int J Greenh Gas Control* **40,** 126–66 (2015)
3. Fernández, J.R, Abanades, J.C. Overview of the Ca–Cu looping process for hydrogen production and/or power generation. *Curr Opin Chem Eng*. **17**, 1–8 (2017)
4. Adanez, J. et al. Progress in chemical-looping combustion and reforming technologies. *Progress in Energy and Combustion Science* **38**, 215–282 (2012).
5. Grasa, G., Diaz, M., Fernández, J.R., Ameiro, A., Brandt, J., Abanades, J.C. Blast Furnace Gas decarbonisation through Calcium Assisted Steel-mill Off-gas Hydrogen production. Experimental and modelling approach. Chemical Engineering Research and Design, **191** (2023) 507–522

*This project has received funding from the European Union's Horizon 2020 research and innovation programme under the Grant Agreement No **884418***

6. Martínez, I., Grasa, G., Murillo, R., Arias, B., Abanades, J.C. Kinetics of calcination of partially carbonated particles in a Ca-looping system for CO_2 capture. *Energy Fuels* **26** (2), 1432-1440 (2012)
7. Zaheer Abbas, S., Fernández, J.R., Amieiro, A., Rastogi, M., Brandt, J., Spallina, V. Lab-scale experimental demonstration of Ca-Cu chemical looping for hydrogen production and in-situ CO_2 capture from a steel mill. *Fuel Processing Technology* **237**, (2022)
8. Fernández, J.R., Abanades, J.C., Diaz, M., Mendez, A., Alonso, M., Grasa, G., et al. The design of the CASOH process pilot to test the decarbonisation of blast furnace gas using the Ca-Cu chemical loop. *Greenh. Gas Control Poster Communication,* (2022)
9. Abanades, J.C., Porter, R., Catalanotti, E., Mahgerefteh, H.Performance analysis of pressure swing adsorption process for carbon-containing off-gas separation in the Steel industry. *Greenh. Gas Control Poster Communication,* (2022)
10. Abanades, J.C., Arias, B., Fernandez, J.R. Vacuum swing calcination process to produce high purity CO_2 from $CaCO_3$. *Patent EP21382495.6* (2021)
11. Abanades, J.C., Arias, B., Fernandez, J.R Steam partial pressure swing calcination process to produce high purity CO_2 from $CaCO_3$. Patent EP22383113 (2022)
12. Hills, A.W.D. The mechanism of the thermal decomposition of calcium carbonate. *Chem Eng Sci*. **23**(4),297–320 (1968)
13. Alarcón, J.M., Fernández, J.R., $CaCO_3$ calcination by the simultaneous reduction of CuO in a Ca/Cu chemical looping process. *Chemical Engineering Science* **137**, 254–267 (2015).
14. Borgwardt, R.H. Calcination Kinetics and Surface Area of Dispersed Limestone Particles. *AIChE J*. **31**,103–11 (1985).
15. Diaz, M. Alonso, M., Grasa,G. Fernandez, J.R.The Ca-Cu looping process using natural CO_2 sorbents in a packed bed: Operation strategies to accommodate activity decay. Chemical Engineering Science **273** (2023)
16. Spallina, V., Chiesa, P., Martelli, E., Gallucci, F., Romano, M.C., Lozza, G., van Sint Annaland, M. Reactor design and operation strategies for a large-scale packed-bed CLC power plant with coal syngas. *Int. J. Greenh. Gas Control* **36**, 34–50 (2015).

*This project has received funding from the European Union's Horizon 2020 research and innovation programme under the Grant Agreement No **884418***